Accepted Manuscript

Efficient synthesis of new antiproliferative steroidal hybrids using the molecular hybridization approach

Bin Yu, Ping-Ping Qi, Xiao-Jing Shi, Ruilei Huang, Hao Guo, Yi-Chao Zheng, De-Quan Yu, Hong-Min Liu

PII: S0223-5234(16)30309-9

DOI: 10.1016/j.ejmech.2016.04.024

Reference: EJMECH 8539

To appear in: *European Journal of Medicinal Chemistry*

Received Date: 18 November 2015

Revised Date: 14 March 2016

Accepted Date: 8 April 2016

Please cite this article as: B. Yu, P.-P. Qi, X.-J. Shi, R. Huang, H. Guo, Y.-C. Zheng, D.-Q. Yu, H.-M. Liu, Efficient synthesis of new antiproliferative steroidal hybrids using the molecular hybridization approach, *European Journal of Medicinal Chemistry* (2016), doi: 10.1016/j.ejmech.2016.04.024.

Steroidal hybrids were synthesized and evaluated for their antiproliferative activity. Compound **12g** potently inhibited growth of SH-SY5Y cells possibly through the inactivation of LSD1, arrested cell cycle at G2/M phase, induced apoptosis and decreased MMP. Docking simulations were performed to rationalize the potency toward LSD1.

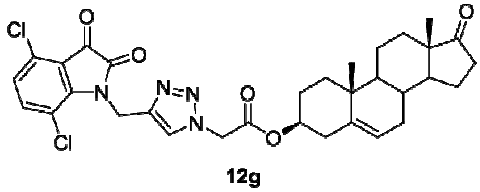

12g

SH-SY5Y IC_{50} = 4.06±0.61 μM
LSD1 IC_{50} = 3.18 μM
First Steroid-Based LSD1 inactivator

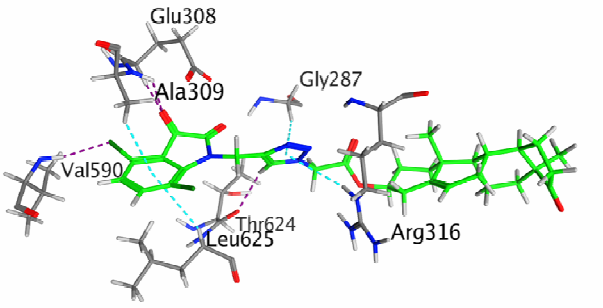

Efficient synthesis of new antiproliferative steroidal hybrids using the molecular hybridization approach

Bin Yu[a, †], Ping-Ping Qi[a, †], Xiao-Jing Shi[a, †], Ruilei Huang[b], Hao Guo[c], Yi-Chao Zheng[a], De-Quan Yu[a, *], Hong-Min Liu[a, *]

[a] *School of Pharmaceutical Sciences & Collaborative Innovation Center of New Drug Research and Safety Evaluation, Zhengzhou University, Zhengzhou 450001, China*

[b] *School of Pharmaceutical Sciences, Central South University, Changsha 410000, China*

[c] *Chongqing Institute of Forensic Science, Chongqing 400021, China*

Abstract: A series of steroidal hybrids with different terminal bioactive scaffolds were synthesized using the molecular hybridization approach and further evaluated for their antiproliferative activity against several cancer cell lines of different origins using the MTT assay. The preliminary results indicated that compounds **12a-h** with the terminal isatin motif were remarkably sensitive to SH-SY5Y cells, thereby exerting potent growth inhibition in vitro. This selectivity is possibly attributed to LSD1 inactivation (IC_{50} = 3.18 μM). Besides, we also found that the chloro atom at the 7-position on the isatin core was beneficial for the activity through the SARs studies. Among this series, compound **12g** showed the best inhibitory activity (IC_{50} = 4.06 μM) against SH-SY5Y cells, which was comparable to that of 5-Fu. Compound **12g** arrested cell cycle at G2/M phase, induced apoptosis accompanied with decrease of mitochondrial membrane potential, and inhibited LSD1 potently (IC_{50} = 3.18 μM). Docking studies showed that compound **12g** formed interactions with surrounding amino acid residues and the steroid nucleus occupied the tubular hydrophobic cavity of the active site. Compounds **13-18** represented weak to moderate activity against the tested cancer cell lines. The steroidal dimer **20** and the structurally simplified non-steroidal dimer **21** were found to be devoid of the inhibitory activity.

Keywords: Steroids; Molecular hybridization; Antiproliferative activity; Apoptosis; Cell cycle arrest; LSD1 inactivation; Docking simulations

1. Introduction

The molecular hybridization generally refers to the incorporation of two or more bioactive fragments into one molecule through suitable linkers. These new hybrids are always endowed with improved activity or new biological properties compared to their individual components. Molecular hybridization, as an emerging concept in drug discovery, has recently gained increasing attention among medicinal community with several successful examples reported by different groups (Fig. 1) [1]. For example, the hybridization of indolinone with tyrosine kinase inhibitor Axitinib developed by Pfizer yielded the first potent PLK4 inhibitor CFI-400945, which has advanced into phase I clinical trials for cancer therapy [2, 3]. Besides, Solaja et al. recently reported that steroidal 4-amino quinolines are potent, dual-target inhibitors of the botulinum neurotoxin serotype A metalloprotease and *P. falciparum* Malaria (K_i = 0.103 μM) [4]. Based on the principle of molecular hybridization, our group recently synthesized two types of selective

* Corresponding authors: Prof. Hong-Min Liu (liuhm@zzu.edu.cn); De-Quan Yu (dqyu@imm.ac.cn); †These authors contributed equally to this work.

LSD1 inhibitors, namely the 1, 2, 3-triazole-dithiocarbamates [5, 6] and pyrimidine-thiourea hybrids [7] as orally active anticancer candidates (IC_{50} = 0.89 and 4.01 μM against MGC-803, respectively).

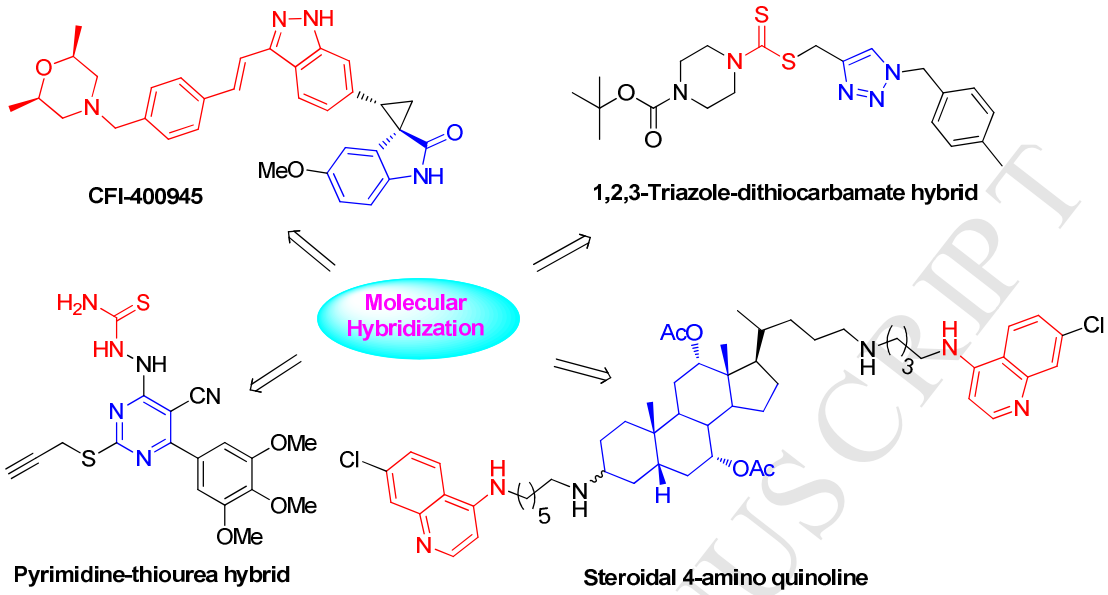

Fig. 1 Representative bioactive molecules designed based on the molecular hybridization principle

Dehydroepiandrosterone (abbreviated as DHEA), an endogenous steroid secreted by the adrenal cortex, is able to inhibit the proliferation of human cancer cells in vitro and in vivo by targeting PI3K/Akt signaling pathway [8]. Given its anticancer potential and readily commercial availability, DHEA was chosen as a starting point for designing new steroidal hybrids with anticancer properties. In order to increase the structural diversity and further investigate the structural requirements for better potency, several different well-known bioactive scaffolds, such as isatins [9-11], chalcones [12] and coumarins [6], were incorporated into the designed hybrids through the molecular hybridization approach. In addition, steroidal hybrids with the terminal phenoxy groups and anilines were also synthesized to compare the activity. As for the spacers, several linkers like polyethylene glycol (PEG) [13], dithiocarbamate [12, 14] and 1, 2, 3-triazole [15, 16] have been extensively used in drug design and, more importantly, have been proved to be crucial for the activity [13, 15]. We herein employed the triazole bridge to link DHEA and biologically active scaffolds mentioned above to generate new steroidal hybrids considering the diverse biological properties and synthetic accessibility of triazoles. We previously reported a novel [1,2,4] triazolo [1,5-*a*] pyrimidine-based phenyl-linked steroid dimer, which represented excellent antiproliferative activity against human cancer cell lines and low toxicity toward human normal cells [17]. As a follow-up work, we designed another new steroid dimer as well using the 5-fluorouracil (5-FU) as the bioactive center based on the molecular hybridization approach. As part of our efforts toward finding new steroidal derivatives with anticancer activity [18-23] , this design, as shown in Fig. 2, would help us gain a deeper insight into the structural requirements for identifying potent steroid-based anticancer agents.

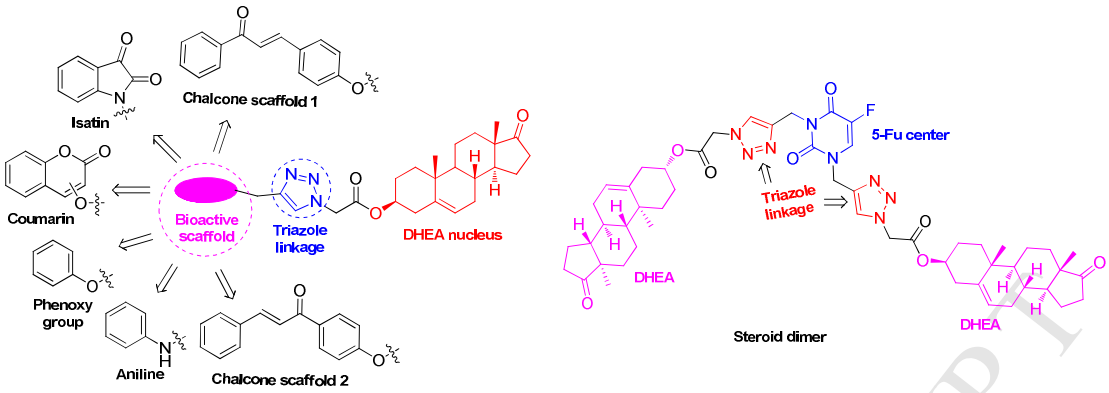

Fig. 2 Designed steroidal hybrids in this work

2. Results and discussion

2.1. Chemistry

2.1.1. Synthesis of dehydroandrosterone azidoacetate **2**

The target molecules can be synthesized from the corresponding alkynes and steroidal azide **2** through the click chemistry. The synthesis of the steroidal azide **2** is shown in Scheme 1. Bromoacetylation of DHEA under Schotten-Baumann conditions [24] afforded the corresponding bromide **1** in 87 % yield, which then reacted with NaN_3 in DMSO to give the steroidal azide **2** in 85 % yield. The steroidal azide **2** was used directly for next step after simple aqueous work-up procedure. In the first step, a two-phase solvent system (DCM/H_2O) was used; the base $NaHCO_3$ in aqueous phase neutralized the generated HBr, while the starting materials and the product were in the organic phase. Besides, this condition avoided unwanted side reactions of bromide **1** with H_2O.

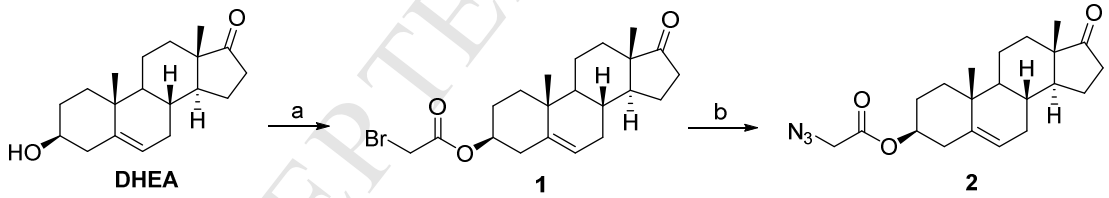

Scheme 1 Synthesis of the steroidal azide **2**. (a) Bromoacetyl bromide, $NaHCO_3$, DCM/H_2O (1/1), rt; (b) NaN_3, DMSO, rt-50 ^oC.

2.1.2. Synthesis of alkyne building blocks **5**-**11**

To increase the structural diversity and further explore the structural requirements, the divergent synthesis focusing on the variation of bioactive scaffolds was employed. Considering the broad and promising bioactivities of chalcones [25-28], coumarins [29-31] and isatin derivatives [9, 10, 32], these scaffolds as illustrated in Fig. 2 were introduced to the steroid nucleus using the molecular hybridization approach. Besides, the phenoxy group and anilines were also introduced as the terminal motifs with an aim of comparing the activity with those hybrids having different bioactive scaffolds. Another consideration of this design is that phenoxy groups and anilines could act differently a H-bond acceptors and donors, respectively to interact with potential targets. Such design could provide us more details about the structural

requirements for better potency, ultimately helping us design more potent steroid-based anticancer agents.

The synthesis of alkyne building blocks is shown in Fig. 3. Treatment of 4-hydroxybenzaldehyde and 4-hydroxyacetophenone with propargyl bromide in the presence of K_2CO_3 gave compounds **3** and **4**, respectively, which then underwent the KF/Al_2O_3-catalyzed Claisen-Schmidt condensations with aromatic aldehydes and acetophenones, affording substituted chalcones **5a-e** and **6a-b**. Similarly, propargyl substituted isatins **7a-h**, coumarins **8a-c**, phenols **9a-c** and anilines **10a-c** were conveniently synthesized in the presence of K_2CO_3 in DMF or acetone. In order to construct 5-Fu linked steroid dimer, dipropargyl substituted 5-Fu **11** was also synthesized.

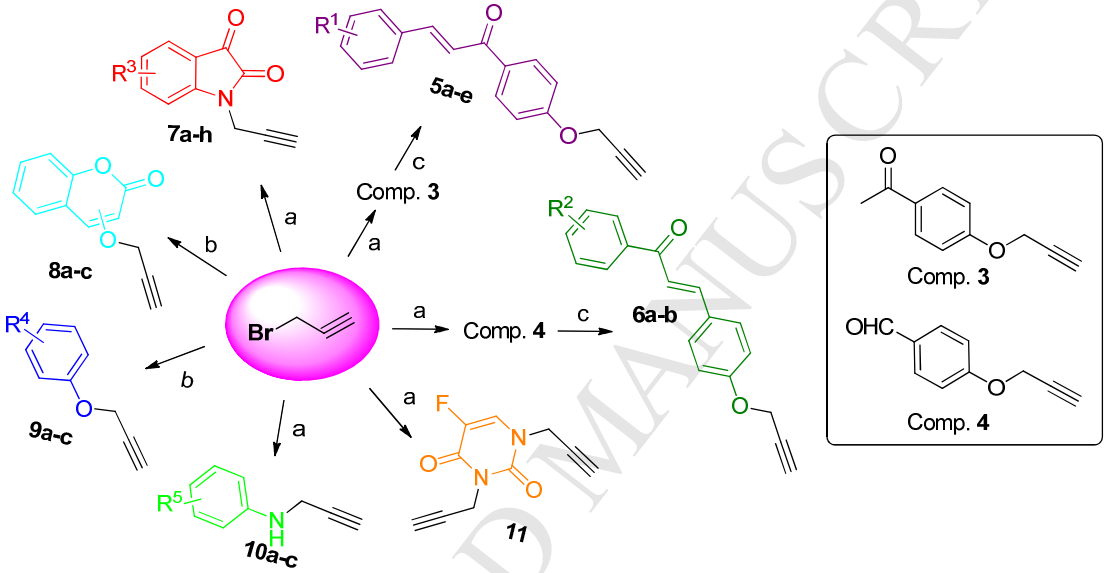

Fig. 3 Synthesis of alkyne building blocks. (a) K_2CO_3, DMF, rt; (b) K_2CO_3, acetone, rt-50 ^oC; (c) Al_2O_3/KF, EtOH, 50 ^oC.

2.1.3. Synthesis of steroidal hybrids **12**-**18**

With the azide and alkyne building blocks in hand, the designed steroidal hybrids were efficiently synthesized through the standard CuAAC reactions in moderate to good yields (Scheme 2).

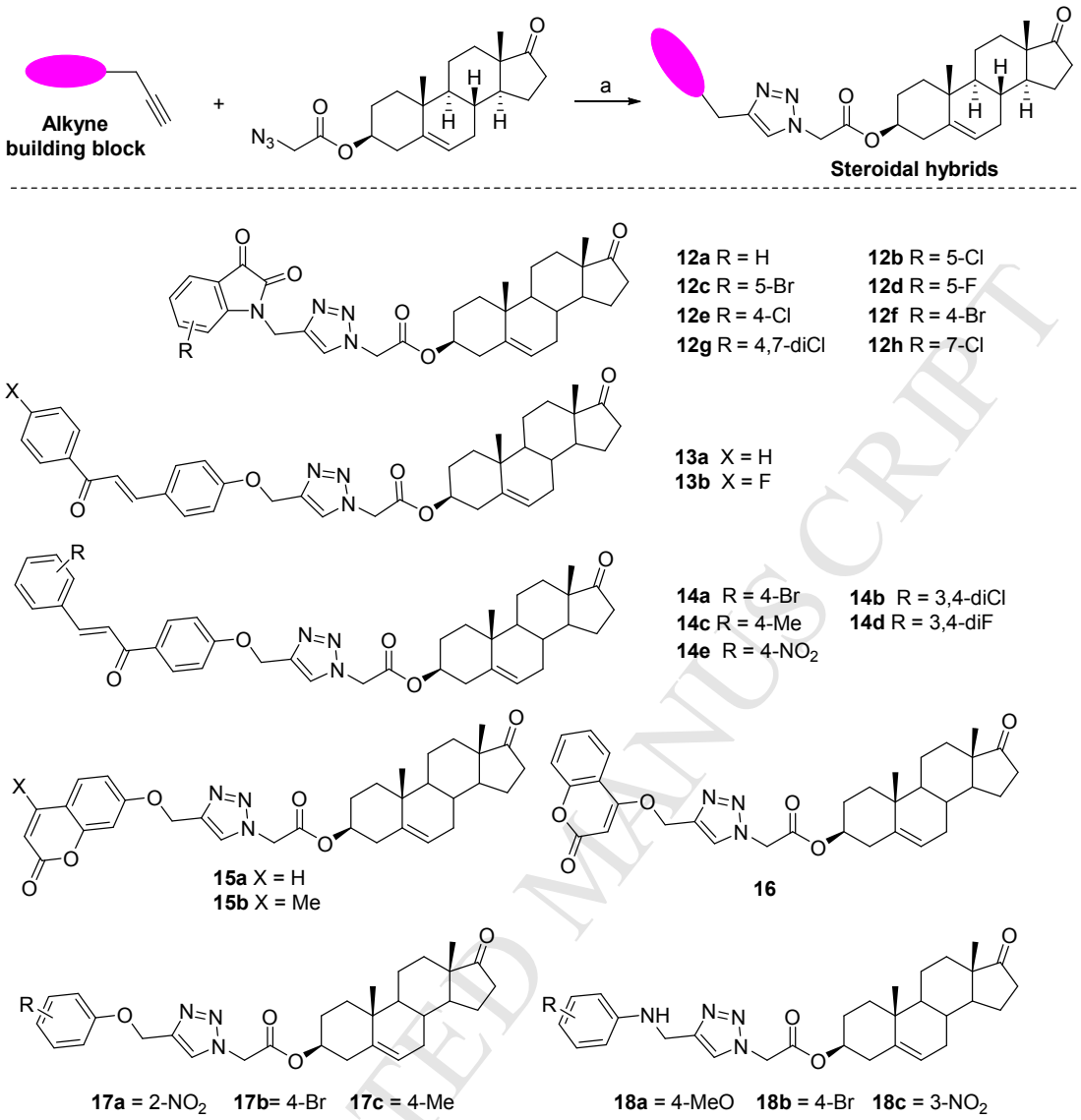

Scheme 2 Synthesis of steroidal hybrids. (a) $CuSO_4 \cdot 5H_2O$, sodium ascorbate, THF/H_2O (1/1), rt.

2.1.4. Synthesis of dimers **20** and **21**

We previously found that steroid dimers possessed excellent antiproliferative activity and low toxicity to normal cells [17]. Inspired by this finding, we also synthesized a new steroid dimer **20** using the 5-Fu as the bioactive center. Besides, structurally simplified compound **21** was synthesized as well from compound **11** and 2-chlorobenzyl azide **19** to compare the antiproliferative activity (Scheme 3).

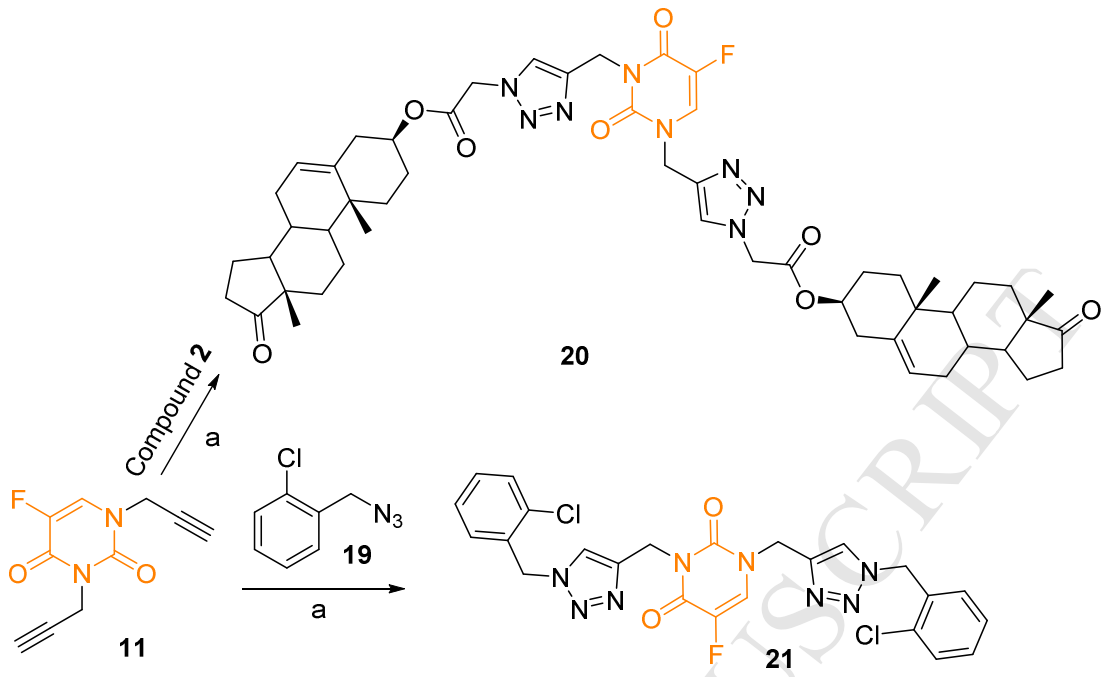

Scheme 3 Synthesis of dimers **20** and **21**. (a) $CuSO_4 \cdot 5H_2O$, sodium ascorbate, THF/H_2O (1/1), rt.

2.2. Antiproliferative activity

In continuation with our efforts toward the identification of novel steroidal compounds with anticancer potential, we evaluated the antiproliferative activity of steroidal hybrids **12a-h**, **13a-b**, **14a-e**, **15a-b**, **16**, **17a-c**, **18a-c**, steroid dimer **20** and compound **21** against several cancer cell lines of different origins (MCF-7, U87, SH-SY5Y, MGC-803 and EC109) using the MTT assay. The well-known anticancer drug 5-fluorouracil (5-Fu) works principally through irreversible inhibition of thymidylate synthase, while some steroidal derivatives such as estradiol, progesterone, DHEA, testosterone have also been reported to be able to markedly inhibit thymidylate synthase [33]. Due to the similar mode of action, 5-Fu was used as the reference drug in the MTT assay. The preliminary results are listed in Table 1.

Table 1 *In vitro* antiproliferative activity of steroidal hybrids

Compound	IC_{50} (μM)				
	MCF-7	U87	SH-SY5Y	MGC-803	EC109
12a	> 128	45.61±1.66	**8.62±0.94**	> 128	> 128
12b	> 128	47.89±1.68	**7.32±0.87**	57.77±1.32	61.72±1.79
12c	> 128	39.21±1.59	**10.3±1.01**	32.49±1.51	44.11±1.65
12d	> 128	91.13±1.96	**9.25±0.97**	58.85±1.77	> 128
12e	> 128	33.07±1.52	**18.51±1.27**	> 128	123.99±2.09
12f	> 128	21.31±0.58	> 128	26.38±1.42	78.35±1.31
12g	**32.25±1.51**	**9.57±0.98**	**4.06±0.61**	**5.95±0.77**	**20.77±1.73**
12h	13.29±1.12	20.82±1.32	14.6±1.16	8.74±0.94	84.61±1.93
13a	> 128	> 128	75.0±1.88	> 128	117.59±2.07
13b	91.47±1.97	> 128	46.45±1.67	> 128	> 128

14a	111.88±2.05	> 128	72.56±1.86	> 128	79.81±1.33
14b	> 128	> 128	36.64±1.56	> 128	> 128
14c	73.34±1.87	> 128	50.06±1.70	> 128	> 128
14d	92.58±1.97	> 128	42.07±1.62	> 128	> 128
14e	> 128	> 128	> 128	99.46±2.00	> 128
15a	> 128	43.71±1.64	54.85±1.74	> 128	> 128
15b	> 128	47.43±1.68	49.47±1.70	> 128	> 128
16	> 128	40.02±1.6	> 128	> 128	> 128
17a	45.12±1.65	> 128	65±1.81	51.34±1.71	49.84±1.70
17b	93.18±1.97	30.13±1.48	22.72±1.36	48.23±1.68	20.99±1.32
17c	38.6±1.59	18.46±1.14	26.95±1.43	21.61±1.34	23.89±1.38
18a	21.27±1.05	96.53±1.42	69.76±1.84	11.56±1.06	24.73±0.85
18b	27.6±1.39	86.72±0.89	59.41±1.77	19.42±1.35	37.12±1.43
18c	45.2±1.12	> 128	> 128	28.62±1.46	55.43±1.84
20	> 128	> 128	> 128	> 128	> 128
21	> 128	> 128	> 128	> 128	> 128
5-Fu	7.61±1.31	5.61±0.37	3.26±0.46	1.25±0.22	3.17±0.43

As shown in Table 1, these hybrids displayed different antiproliferative activities against different cancer cell lines with the IC_{50} values ranging from 4.06 to > 128 μM. For compounds **12a-h** with the terminal isatin scaffold, their antiproliferative activities varied significantly toward different cancer cell lines. For SH-SY5Y cells, compounds **12a-e** and **12g-h** showed excellent inhibition of cell growth (IC_{50} < 20 μM), a slight difference in inhibiting growth of SH-SY5Y cells was observed for compounds with different substitution patterns. Among them, compound **12g** with the 4, 7 -dichloro group showed the best antiproliferative activity with an IC_{50} value of 4.06 μM, which was comparable to that of 5-Fu (IC_{50} = 3.26 μM), while compounds **12e** (4-Cl) and **12h** (7-Cl) exhibited slightly decreased inhibitory activity with the IC_{50} values of 18.51 and 14.6 μM, respectively. However, compound **12f** with a bromine atom at the 4-positin was found to be devoid of the activity (IC_{50} > 128 μM). Besides, compounds **12g-h** showed moderate to good antiproliferative activity against the tested cancer cell lines. By contrast, compounds **12a-f** acted differently toward different cancer cell lines. Most of these compounds had moderate inhibitory activity against U87, MGC-803 and EC109 cells, while no activity was observed toward MCF-7 cells for compounds **12a-f** (IC_{50} > 128 μM). This observation suggests that these compounds may act through targeting specific biological targets that are overexpressed in certain cells. By comparing the activity of compounds **12e** and **12g-h**, we may conclude that 7-chloro or 4, 7-dichloro substituent is beneficial for improving the activity, at least against SH-SY5Y cells. Another interesting finding is that SH-SY5Y cells were more sensitive to compounds **12a-h**, which is probably attributed to the isatin motif. This observation is consistent with the recent findings by Hou et al. [34, 35]. They reported that isatin itself can significantly inhibit the growth of SH-SY5Y cells in vitro and in vivo and induce apoptosis via the mitochondrial pathway. In addition to aforementioned optimizations, further modifications could be carried out to design more potent compounds based on the high reactivity of C3 carbonyl group of isatin. This finding together with the preliminary mechanism reported by Hou et al. [34, 35] would provide a basis for designing more potent molecules selectively targeting SH-SY5Y cells.

By contrast, compounds **13a-b** and **14a-e** with the terminal chalcone scaffold in place of the isatin motif showed moderate but remarkably decreased inhibitory activity against SH-SY5Y cells with the IC_{50} values more than 36.64 μM compared to compounds **12a-h**. Compounds **13a-b** and **14a-e** exerted weak or no activity toward other cancer cell lines regardless of their substituent patterns and the nature of substituents. Similarly, compounds **15a-b** and **16** with the terminal coumarin scaffold exhibited moderate inhibitory activity against U87 and SH-SY5Y cells with the IC_{50} values ranging from 40.02 to > 128 μM, while no activity was observed for MCF-7, MGC-803 and EC109 cells (IC_{50} > 128 μM). The difference may be attributed to the poor membrane permeability of compounds with the chalcone and coumarin scaffolds. Interestingly, when the phenoxy and aniline groups were introduced instead of the well-known bioactive chalcone and coumarin scaffolds, compounds **17** and **18** showed significantly improved growth inhibition toward MCF-7, MGC-803 and EC109 cells. Among them, compound **18a** was the most potent one with an IC_{50} value of 11.56 μM against MGC-803. However, compounds **18a-c** with the terminal aniline group exhibited weak or no activity against U87 and SH-SY5Y cells.

5-Fu is a frequently used chemotherapeutic agent for the treatment of solid tumors acting through inhibiting thymidylate synthase. However, its severe side effects such as the high toxicity, poor tumor selectivity, etc, to some extent, have restricted its clinical applications [36]. Therefore, the design and synthesis of new 5-Fu derivatives is necessary to reduce the side effects, while retaining its anticancer potency. There is evidence that *N*1 and/or *N*3 substituted 5-Fu derivatives represent improved antitumor activity and lower toxicity [37]. Additionally, DHEA has also been proved to be able to markedly inhibit thymidylate synthase [33]. So the incorporation of DHEA and 5-Fu into one molecule through suitable linkage would be an effective strategy to design new hybrids with synergistic antitumor effects. On the basis of our previous observations that steroid dimers have excellent antiproliferative activity against cancer cell lines and low toxicity toward non-cancerous cells [17], herein we designed another new steroidal dimer **20**, incorporating 5-Fu and DHEA into one molecule through the triazole linkage. In order to compare the activity, the non-steroidal dimer **21** was also designed and synthesized using the 2-nitrophenyl group in place of DHEA nucleus. Unfortunately, these two dimers **20** and **21** did not show any inhibitory activity toward the tested cancer cells regardless of their substituents attached (IC_{50} > 128 μM). This finding may suggest that it is not a feasible strategy to design potent anticancer agents through installing the triazole group to both nitrogen atoms of 5-Fu.

From above discussions, we can conclude that most of these hybrids exhibited weak to moderate or even no activity against the tested cell lines. However, we observed that compounds **12a-h** with the terminal isatin core were more sensitive to SH-SY5Y cells with excellent inhibitory activity. Among them, compound **12g** was the most potent one with an IC_{50} value of 4.06 μM. These findings provided us some useful information regarding the structural requirements for better potency and would help us design more potent small molecules selectively targeting SH-SY5Y cells.

2.3. Analysis of cell cycle distribution

Tumor cells, relative to normal cells, always grow uncontrollably because of the overexpression of

cyclins or inactivation of critical CDKIs. Targeting the cell cycle of tumor cells has been recognized as a promising strategy for cancer therapy [38]. To determine the effect of our designed steroidal hybrids on the cell cycle, compound **12g** was chosen for this purpose considering its excellent growth inhibition toward SH-SY5Y cells. After treating SH-SY5Y cells with compound **12g** at different concentrations (0, 1.25, 2.5, 5.0 μM) for 24 h, cells were then fixed and stained with PI for flow cytometry analysis. As shown in Fig. 4B, compound **12g** arrested cell cycle at G2/M phase in a concentration-dependent manner, along with decrease of cells in other phases. A representative example is shown in Fig. 4A. The percentage of cells at G2/M phase was increased to 27.74 % at high concentration (5.0 μM) from 14.53 % for the control group.

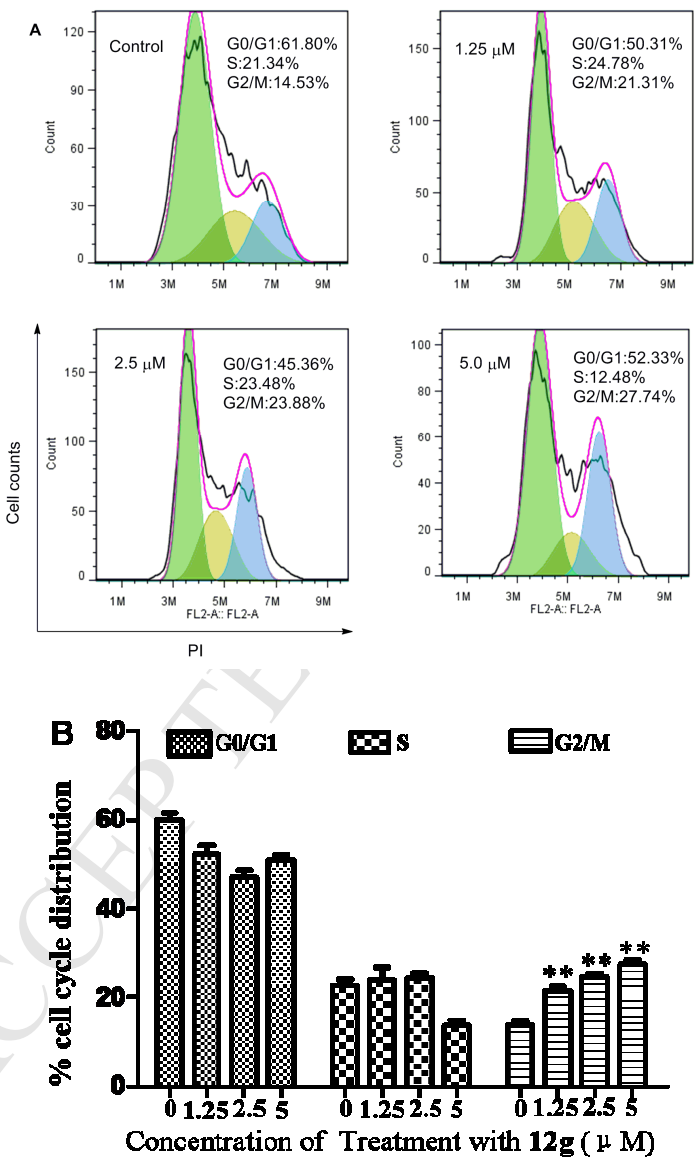

Fig. 4 Effect of compound **12g** on the cell cycle distribution of SH-SY5Y cells. Cells were treated at different concentrations (0, 1.25, 2.5, 5.0 μM) for 24 h. Then the cells were fixed and stained with PI to analyze DNA content by flow cytometry. The experiments were performed three times. (A) Representative example. (B) Quantitative analysis of cell cycle distribution induced by compound **12g**. $^{**}P < 0.01$ was considered statistically significant.

2.4. Apoptosis and possible mechanism involved

The excellent inhibitory activity of compound **12g** against SH-SY5Y cells promoted us to further investigate its apoptotic effect by a biparametric cytofluorimetric analysis using propidium iodide (PI) and Annexin V-FITC. After treating SH-SY5Y cells with compound **12g** at different concentrations (0, 1.25, 2.5, 5.0, 10.0 20.0 μM) for 24 h, cells were labeled with two dyes, and then the flow cytometry was employed to detect the resulting red (PI) and green (FITC) fluorescence. As illustrated in Fig. 5B, compound **12g** induced apoptosis of SH-SY5Y cells in a concentration-dependent manner, especially the late apoptosis. Specifically, the percentage of apoptotic cells was about 9 % for the control group. When treated at 10 or 20 μM, a complete apoptosis was observed with the percentage of apoptosis up to 98.7 % and 98.3 %, respectively. The percentage of the late apoptosis was remarkably increased to 65.7 % when treated at 20 μM from 5.7 % for the control group.

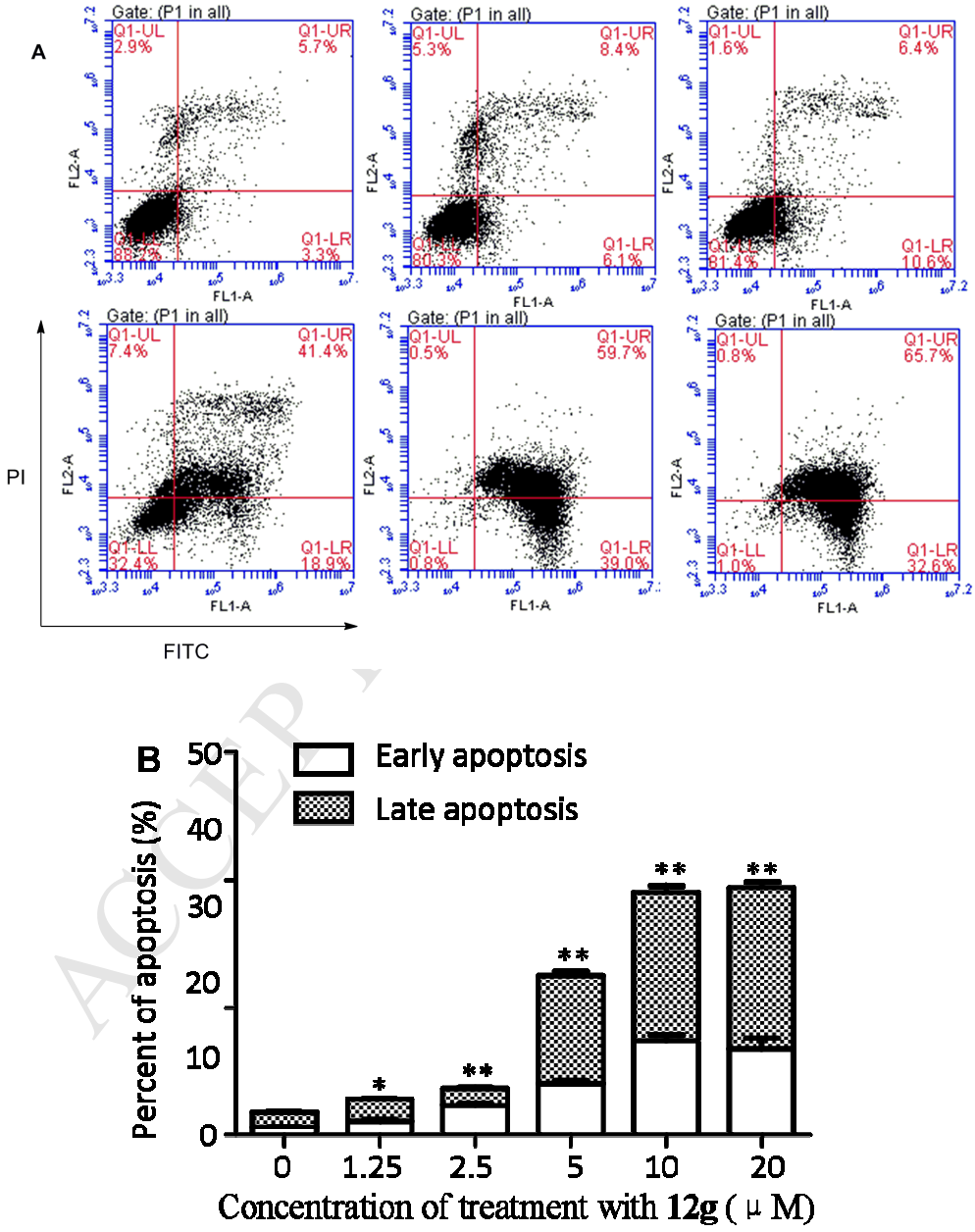

Fig. 5 Apoptotic effect of compound **12g** on SH-SY5Y cells. Apoptotic cells were detected with Annexin V-FITC/PI double staining after incubation at the indicated concentrations for 24 h. The

lower left quadrants represent live cells, the lower right quadrants are for early apoptotic cells, upper right quadrants are for late apoptotic cells, while the upper left quadrants represent cells damaged during the procedure. (A) Representative experiment. (B) Quantitative analysis of apoptotic cells. $^{**}P < 0.01$ was considered statistically significant. The experiments were performed three times.

The decrease of mitochondrial membrane potential (MMP) through multiple mechanisms including deficiency of oxidizable substrates for the mitochondria, blockage of respiration, or uncoupling of the inner membrane, followed by cytochrome c release from the mitochondria and expression changes of apoptosis-related proteins (e.g. Bax, Bcl-2, p53, etc) have been observed during apoptosis [39]. The remarkable apoptosis induced by compound **12g** promoted us to explore whether this compound had an effect on the MMP. SH-SY5Y cells were incubated at the indicated concentrations for 24 h and then stained and analyzed by flow cytometry. As shown in Fig. 6, compound **12g** caused the MMP change in a concentration-dependent manner. The percentage of cells at 10 μM was 40.1 %, significantly higher than that of the control group (5.1 %). A similar result was obtained previously in our group, showing that steroids can decrease the MMP, promote the cytochrome c release, and induce expression changes of related proteins [17]. Therefore, we did not duplicate this work to analyze the expression of proteins by Western blotting analysis but turned our attention to the selectivity observed toward SH-SY5Y cells. Previously, Hou and co-workers proved that isatin can induce apoptosis and inhibit the growth of SH-SY5Y neuroblastoma cells via the mitochondrial pathway [34, 35]. However, the detailed molecular mechanism remains unclear. In SH-SY5Y cells, the lysine-specific demethylase 1 (LSD1) is always overexpressed. Inhibition of LSD1 has been proved to be capable of inhibiting growth of tumors expressing LSD1 in vitro and in vivo [40]. As part of our ongoing efforts toward identifying novel LSD1 inactivators for cancer therapy [5-7, 41], we are interested in investigating whether the observed selectivity of compounds **12a-h** toward SH-SY5Y cells is due to the inhibition of LSD1. To our delight, compound **12g** inhibited LSD1 at low micromolar level (IC_{50} = 3.18 μM). This finding suggests that compounds **12a-h** may inhibit growth of SH-SY5Y cells by inactivating LSD1. To the best of our knowledge, this is the first report about steroid-based LSD1 inhibitors. Further mechanistic studies are ongoing in our laboratories and will be reported in due course.

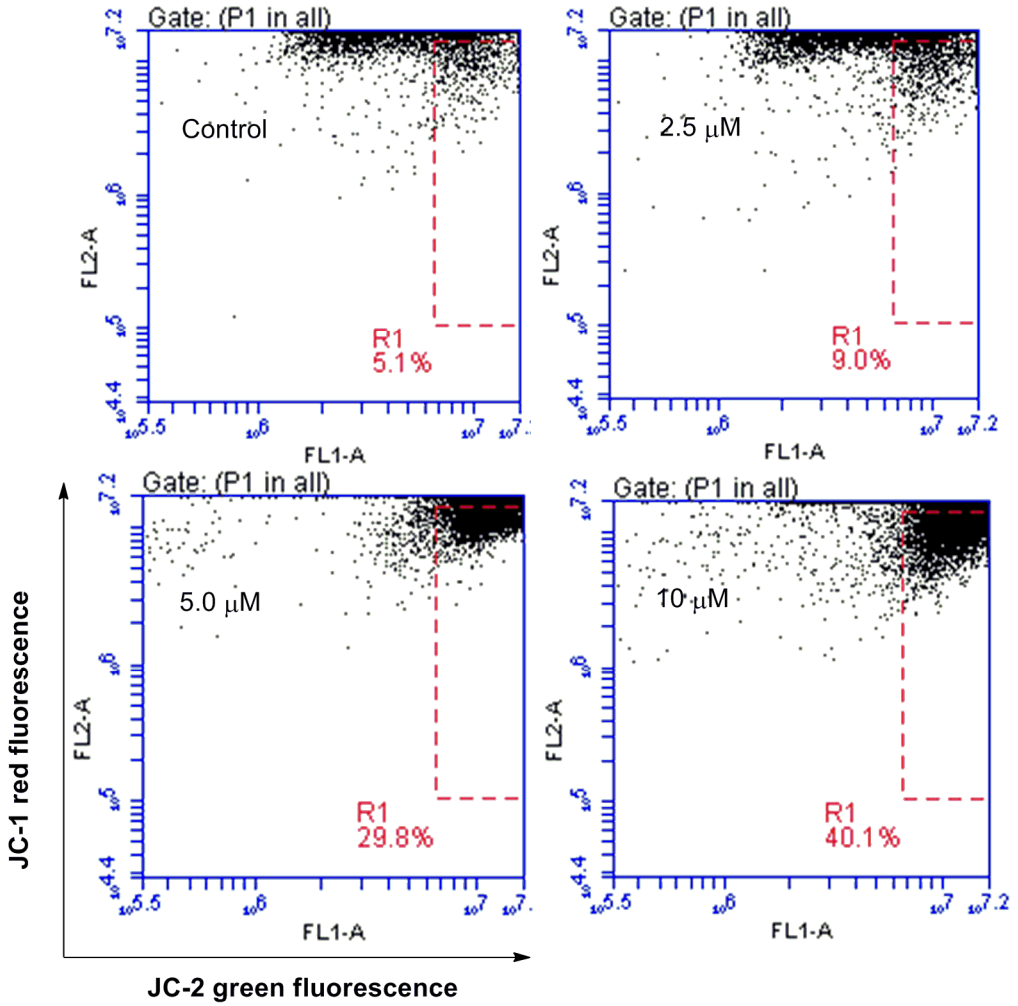

Fig. 6 Changes of mitochondrial membrane potential induced by compound **12g**. SH-SY5Y cells were incubated at the indicated concentrations for 24 h. The cells were stained with JC-1 and then analyzed by flow cytometry.

2.5. Molecular docking studies

In view of the observed good inhibition of compound **12g** toward LSD1, docking simulations were performed to rationalize the potency using the MOE2014 software (PDB code: 2H94) [49]. As shown in Fig. 7A, the C3 carbonyl oxygen of the isatin motif formed hydrogen bonds with Ala309 and Glu308 residues, while the chlorine atom attached to the C4 position of the isatin motif formed C-Cl···H interaction with Val590, which may explain the observed importance of the C4 chlorine atom for the activity. Additionally, the phenyl ring of the isatin motif formed arene-H interactions with Ala309 and Leu625, respectively. The triazole ring also contributed to the activity by forming hydrogen bond with the backbone carbonyl oxygen of Thr624 and arene-H interactions with Gly287 and Arg316 residues. As shown in Fig. 7B, the steroid nucleus of compound **12g** (shown in orange stick) well occupied the tubular hydrophobic cavity in the active site of LSD1, while compound **22** (LSD1 IC_{50} > 10 μM) failed to occupy the hydrophobic cavity, highlighting the importance of the steroid nucleus of compound **12g** in the LSD1 inhibition and also explaining the weak activity of compound **22**. The docking results may help us gain a deeper insight into the SARs studies and provide basis for further optimization.

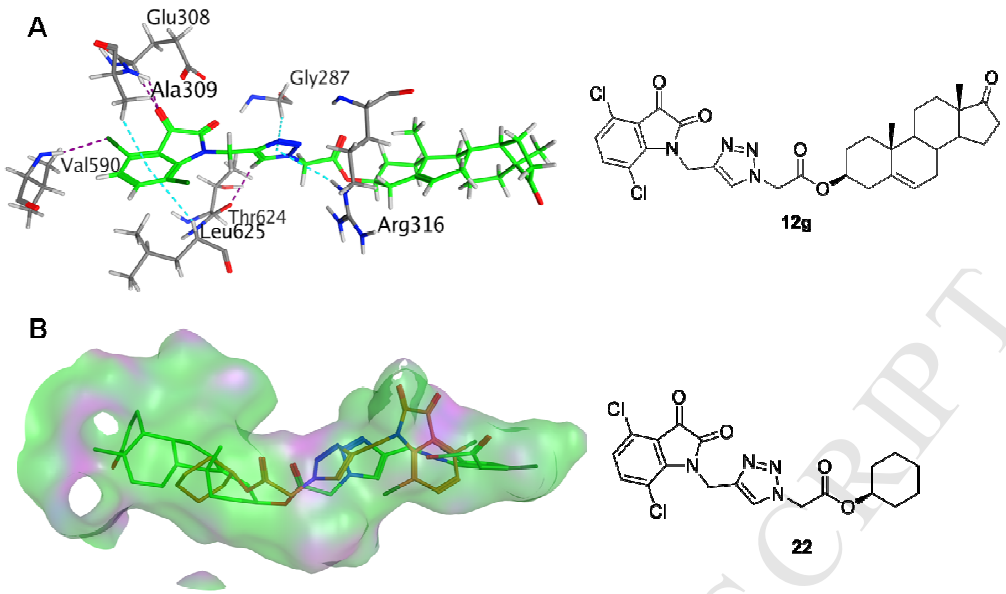

Fig. 7 (A) Predicted binding modes of compound **12g** in the FAD-binding site of LSD1. FAD-binding site residues are colored in gray while compound **12g** is colored in blue and green, respectively. Hydrogen bonds between the protein and compound **12g** are shown in magenta dash line and arene-H interactions are shown in cyan; (B) Putative binding modes of compound **12g** (shown in green stick) and compound **22** (shown in orange stick) in the active sites of LSD1 on the pocket surface (green represents for hydrophobic area, blue represents for mild polar area and magenta for H-bonding).

3. Conclusions

In summary, we designed and synthesized a series of steroidal hybrids with different terminal bioactive scaffolds through the molecular hybridization strategy. The MTT assay showed that most of these hybrids had weak to moderate activity against the tested cancer cell lines. However, steroidal hybrids **12a-h** with the terminal isatin moiety were more sensitive toward SH-SY5Y cells possibly because of the inhibition of LSD1. Besides, compounds **12g-h** with 4, 7-dichloro and 7-chloro groups, respectively also showed moderate to good inhibitory activity against all the tested cancer cell lines. Compound **12g** arrested cell cycle at G2/M phase, induced apoptosis, accompanied the decrease of mitochondrial membrane potential, and inhibited LSD1 potently. Docking simulations indicated that the steroid nucleus played a determinant role in LSD1 inactivation. Additionally, steroid dimer **20** and the structurally simplified compound **21** did not show any inhibitory activity against the tested cancer cells. Further mechanistic studies on the selectivity toward SH-SY5Y cells are ongoing in our laboratories and will be reported in due course.

4. Experimental section

4.1. General

Reagents were purchased and used without further purification. Thin layer chromatography (TLC) was carried out on glass plates coated with silica gel and visualized by UV light (254 nm). Melting points were determined on an X-5 micromelting apparatus. All the NMR spectra were recorded with a Bruker DPX 400 MHz spectrometer with TMS as the internal standard in $CDCl_3$ or DMSO-*d*6.

Chemical shifts are given as δ ppm values relative to TMS (Most of the peaks due to the steroidal skeleton are merged and could not be differentiated. Thus, the δ values of only those peaks that distinguish the product and could easily be differentiated are reported). High-resolution mass spectra of all new compounds were recorded on a Waters Micromass Q-T of Micromass spectrometer by electrospray ionization (ESI). **CAUTION**: Particular care should be taken to avoid grinding sodium azide and acidifying mixtures containing sodium azide because the azide ion can react with acids to form the extremely explosive, volatile and toxic hydrazoic acid. Besides, sodium azide can also form highly explosive salts with many transition metals. Halogenated solvents such as dichloromethane and chloroform should be avoided for sodium azide-involved reactions and subsequent work-up procedures because such solvents can form extremely explosive di- and triazidomethanes with sodium azide [42, 43].

4.2. Synthesis of bromoacetyl DHEA **1**

To a solution of DHEA (1.0 g, 3.47 mmol, 1.0 eq) and $NaHCO_3$ (582 mg, 6.94 mmol, 2.0 eq) in a mixture of DCM (10 mL) and H_2O (10 mL) was added bromoacetyl bromide (934 µL, 10.41 mmol, 3.0 eq) dropwise at room temperature. The mixture was then stirred for about 6 h. Upon completion, the organic layer was separated and the aqueous later was extracted with DCM, the combined organic layers were washed with brine and dried over $MgSO_4$. The solvent was removed under vacuum. The residue was then recrystallized from EtOH to afford the white solid, 1.24 g, yield: 87%, m. p.: 156.1-157.3 ^{o}C, R_f = 0.60 (petroleum ether/ethyl acetate = 2/1), ^{1}H NMR (400 MHz, $CDCl_3$) δ 5.44 (d, *J* = 4.9 Hz, 1H), 4.70 (tdd, *J* = 10.7, 6.5, 4.2 Hz, 1H), 3.83 (s, 2H), 1.07 (s, 3H), 0.91 (s, 3H).^{13}C NMR (100 MHz, $CDCl_3$) δ 166.68, 139.47, 122.33, 75.85, 51.68, 50.10, 47.52, 37.73, 36.81, 36.71, 35.84, 31.45, 31.39, 30.78, 27.43, 26.34, 21.88, 20.33, 19.34, 13.55. HRMS (ESI): *m*/*z* calcd for $C_{21}H_{29}BrNaO_3$ $(M + Na)^+$, 431.1198; found, 431.1180 (Br^{79}) and 433.1161 (Br^{81})

4.3. Synthesis of azidoacetyl DHEA **2**

To a solution of bromoacetyl DHEA (compound **1**, 500 mg, 1.23 mmol, 1.0 eq) in DMSO (10 mL) was added NaN_3 (96 mg, 1.48 mmol, 1.2 eq) at room temperature, and then the mixture was heated to 50 ^{o}C and kept at this temperature for about 3 h. When cooled to room temperature, EtOAc and H_2O were added to the above mixture, the aqueous layer was extracted with EtOAc, the combined layers were washed with H_2O for several times to remove the DMSO, and then washed with brine, dried over $MgSO_4$ and evaporated to give the product, which was pure enough and used directly for next step without further purification. White solid, 385 mg, yield: 85 %, m. p.: 144.9-146.5 ^{o}C, R_f = 0.60 (petroleum ether/ethyl acetate = 2/1). ^{1}H NMR (400 MHz, $CDCl_3$) δ 5.42 (d, *J* = 4.7 Hz, 1H), 4.72 (tt, *J* = 10.9, 5.3 Hz, 1H), 3.84 (s, 2H), 1.05 (s, 3H), 0.88 (s, 3H).^{13}C NMR (100 MHz, $CDCl_3$) δ 167.72, 139.41, 122.39, 75.61, 51.67, 50.50, 50.09, 47.51, 37.94, 36.82, 36.70, 35.83, 31.43, 31.38, 30.77, 27.63, 21.88, 20.32, 19.32, 13.55. HRMS (ESI): *m*/*z* calcd for C21H29N3NaO3 $(M + Na)^+$, 394.2107; found, 394.2095.

4.4. General procedure for the preparation of propargyl substituted isatin derivatives **7a-h**

To a solution of isatin derivative (0.68 mmol, 1.0 eq) in DMF (4 mL) was added K_2CO_3 (0.68 mmol, 1.0 eq) at room temperature, the mixture was stirred for about 30 min, and then the propargyl bromide (0.75 mmol, 1.1 eq) was added dropwise. The mixture was stirred for 6-10 h at room temperature depending on the isatin derivative used. Upon completion, EtOAc and H_2O were

added. The aqueous layer was extracted with EtOAc; the combined organic layers were washed with H_2O for several times to remove the DMF, and then washed with brine, dried over $MgSO_4$ and evaporated to give the products.

4.4.1. *N*-Propargyl isatin **7a**, jacinth solid, yield: 82 %, m. p.: 159.3-160.5 ^{o}C, R_f =0.59 (petroleum ether/ethyl acetate = 2/1). ^{1}H NMR (400 MHz, $CDCl_3$) δ 7.66 (dd, *J* = 12.3, 4.5 Hz, 2H), 7.25 – 7.06 (m, 2H), 4.54 (d, *J* = 2.5 Hz, 2H), 2.32 (t, *J* = 2.5 Hz, 1H).^{13}C NMR (100 MHz, $CDCl_3$) δ 182.55, 157.17, 149.62, 138.46, 125.47, 124.22, 117.68, 111.12, 75.69, 73.36, 29.46.

4.4.2. *N*-Propargyl-5-chloroisatin **7b**, saffron solid, yield: 75 %, m. p.: 168.4-169.7 ^{o}C, R_f = 0.61(Petroleum ether/ethyl acetate = 2/1). ^{1}H NMR (400 MHz, $CDCl_3$) δ 7.70 – 7.57 (m, 2H), 7.13 (dd, *J* = 7.9, 1.0 Hz, 1H), 4.56 (d, *J* = 2.5 Hz, 2H), 2.35 (t, *J* = 2.5 Hz, 1H).^{13}C NMR (100 MHz, $CDCl_3$) δ 181.57, 156.60, 147.85, 137.83, 130.12, 125.36, 118.49, 112.48, 75.29, 73.77, 29.61.

4.4.3. *N*-Propargyl-5-bromoisatin **7c**, red solid, yield: 86 %, m. p.: 160.3-162.0 ^{o}C, R_f = 0.42 (petroleum ether/ethyl acetate = 2/1). ^{1}H NMR (400 MHz, $CDCl_3$) δ 7.77 (m, 2H), 7.08 (dd, *J* = 7.9, 0.9 Hz, 1H), 4.55 (d, *J* = 2.5 Hz, 2H), 2.35 (t, *J* = 2.5 Hz, 1H).^{13}C NMR (100 MHz, $CDCl_3$) δ 181.40, 156.42, 148.29, 140.67, 128.24, 118.84, 117.17, 112.87, 75.25, 73.80, 29.60.

4.4.4. *N*-Propargyl-5-fluoroisatin **7d**, red solid, yield: 73 %, m. p.: 128.5-129.9 ^{o}C, R_f = 0.60 (petroleum ether/ethyl acetate = 2/1).^{1}H NMR (400 MHz, $CDCl_3$) δ 7.47 – 7.31 (m, 2H), 7.14 (dd, *J* = 8.5, 3.6 Hz, 1H), 4.55 (d, *J* = 2.5 Hz, 2H), 2.35 (t, *J* = 2.5 Hz, 1H).^{13}C NMR (100 MHz, $CDCl_3$) δ 182.02 ($J_{C\text{-}F}$ = 2.2 Hz), 159.54 ($J_{C\text{-}F}$ = 246.4 Hz), 156.94 ($J_{C\text{-}F}$ = 1.5 Hz), 145.68 ($J_{C\text{-}F}$ = 2.1 Hz), 124.85 ($J_{C\text{-}F}$ = 24.2 Hz), 118.28 ($J_{C\text{-}F}$ = 7.1 Hz), 112.54 ($J_{C\text{-}F}$ = 11.5 Hz), 112.38 ($J_{C\text{-}F}$ = 5.6 Hz), 75.41, 73.68, 29.58.

4.4.5. *N*-Propargyl-4-chloroisatin **7e**, saffron solid, yield: 89 %, m. p.: 148.3-149.8 ^{o}C, R_f = 0.31 (petroleum ether/ethyl acetate = 2/1). ^{1}H NMR (400 MHz, $CDCl_3$) δ 7.58 (t, *J* = 8.1 Hz, 1H), 7.14 (d, *J* = 8.2 Hz, 1H), 7.06 (d, *J* = 7.9 Hz, 1H), 4.56 (d, *J* = 2.5 Hz, 2H), 2.35 (t, *J* = 2.5 Hz, 1H).^{13}C NMR (100 MHz, $CDCl_3$) δ 179.41, 156.27, 150.64, 138.62, 133.96, 125.79, 114.80, 109.38, 75.38, 73.69, 29.65.

4.4.6. *N*-Propargyl-4-bromoisatin **7f**, yellow solid, yield: 89 %, m. p.: 153.1-154.9 ^{o}C, R_f = 0.26 (petroleum ether/ethyl acetate = 2/1). ^{1}H NMR (400 MHz, $CDCl_3$) δ 7.49 (t, *J* = 8.0 Hz, 1H), 7.33 (d, *J* = 8.1 Hz, 1H), 7.11 (d, *J* = 7.9 Hz, 1H), 4.57 (d, *J* = 2.5 Hz, 2H), 2.34 (t, *J* = 2.5 Hz, 1H).^{13}C NMR (100 MHz, $CDCl_3$) δ 179.90, 156.21, 151.10, 138.42, 128.93, 121.74, 116.52, 109.86, 75.36, 73.67, 30.94, 29.53.

4.4.7. *N*-Propargyl-4, 7-dichloroisatin **7g**, saffron solid, yield: 76 %, m. p.: 151.8-153.3 ^{o}C, R_f = 0.52 (petroleum ether/ethyl acetate = 2/1). ^{1}H NMR (400 MHz, $CDCl_3$) δ 7.51 (d, *J* = 8.7 Hz, 1H), 7.10 (d, *J* = 8.7 Hz, 1H), 4.94 (d, *J* = 2.4 Hz, 2H), 2.34 (t, *J* = 2.4 Hz, 1H).^{13}C NMR (100 MHz, $CDCl_3$) δ 178.68, 157.00, 146.19, 140.48, 133.05, 126.79, 117.16, 116.11, 77.22, 73.27, 31.94.

4.4.8. *N*-Propargyl-7-chloroisatin **7f**, brown solid, yield: 88 %, m. p.: 151.7-152.4 ^{o}C, R_f =

0.47(petroleum ether/ethyl acetate = 2/1). ^{1}H NMR (400 MHz, $CDCl_3$) δ 7.67 – 7.54 (m, 2H), 7.22 – 7.09 (m, 1H), 4.93 (d, *J* = 2.5 Hz, 2H), 2.33 (t, *J* = 2.5 Hz, 1H).^{13}C NMR (100 MHz, $CDCl_3$) δ 181.76, 157.88, 145.28, 140.55, 125.21, 124.18, 120.60, 117.95, 77.50, 72.94, 31.84.

4.5. Preparation of propargyloxy substituted chalcones **5a-e** and **6a-b**

4.5.1. Synthesis of 4-propargyloxy benzaldehyde **4**

To a stirred solution of 4-hydroxybenzaldehyde (500 mg, 4.10 mmol, 1.0 eq) in DMF (10 mL) was added K_2CO_3 (566 mg, 4.10 mmol, 1.0 eq). 30 min later, propargyl bromide (654 μL, 8.20 mmol, 2.0 eq) was added dropwise at room temperature. The mixture was stirred for about 6-10 h. Upon completion, EtOAc and H_2O were added, the aqueous layer was extracted with EtOAc, the combined organic layers were washed with H_2O for several times to remove the DMF, and the organic layers were then washed with brine, dried over $MgSO_4$ and evaporated to give the product. White solid, yield: 77 %, m. p.: 82.3-83.4 ^{o}C, R_f = 0.55 (petroleum ether/ethyl acetate = 2/1). ^{1}H NMR (400 MHz, $CDCl_3$) δ 9.93 (s, 1H), 7.88 (d, *J* = 8.7 Hz, 2H), 7.12 (d, *J* = 8.7 Hz, 2H), 4.81 (d, *J* = 2.3 Hz, 2H), 2.60 (t, *J* = 2.3 Hz, 1H).^{13}C NMR (100 MHz, $CDCl_3$) δ 190.79, 162.38, 131.91, 130.61, 115.19, 77.55, 76.38, 55.96.

4.5.2. General procedure for the synthesis of 4-propargyloxy chalcones **6a-b**

To a solution of aldehyde (0.66 mmol, 1.0 eq) and acetophenone (0.79 mmol, 1.2 eq) in EtOH (4 mL) was added KF/Al_2O_3 (0.66 mmol, 1.0 eq), which was prepared following our previous reported method [17]. The mixture was kept at 50 ^{o}C for 5-6 h. Upon completion, the catalyst was filtered and the residue was thoroughly washed with DCM, the solvent was removed under reduced pressure to afford the products, which were used without further purification. Compounds **6a-b** have been reported previously [44], so the NMR data are not given here.

4.5.3. Synthesis of 4-propargyloxy acetophenone **3**

To a solution of 4-hydroxyacetophenone (700 mg, 5.14 mmol, 1.0 eq) in DMF (12 mL) was added K_2CO_3 (696 mg, 5.14 mmol, 1.0 eq) at room temperature, 30 min later, propargyl bromide (805 μL, 10.28 mmol, 2.0 eq) was added dropwise. The mixture was stirred for 10 h at 35 ^{o}C. Upon completion, EtOAc and H_2O were added, the aqueous layer was extracted with EtOAc, the combined organic layers were washed with H_2O for several times to remove DMF, and the organic layers were washed with brine, dried over $MgSO_4$ and evaporated to give the residue, which was then purified by column chromatography. Light yellow solid, yield: 79 %, m. p.: 77.2-78.0 ^{o}C, R_f = 0.52 (petroleum ether/ethyl acetate = 2/1). ^{1}H NMR (400 MHz, $CDCl_3$) δ 7.98 (d, *J* = 9.0 Hz, 1H), 7.04 (d, *J* = 9.0 Hz, 1H), 4.78 (d, *J* = 2.4 Hz, 1H), 2.70 – 2.44 (m, 4H, -C<u>H</u>$_3$ and ≡C<u>H</u>).^{13}C NMR (100 MHz, $CDCl_3$) δ 196.74, 161.28, 131.06, 130.53, 114.58, 77.76, 76.16, 55.85, 26.40.

4.5.4. General procedure for the synthesis of 4-propargyloxy chalcones **5a-e**

To a solution of aldehyde (0.60 mmol, 1.05 eq) and acetophenone (0.57 mmol, 1.0 eq) in EtOH (4 mL) was added KF/Al_2O_3 (0.57 mmol, 1.0 eq), the mixture was kept at 50 ^{o}C for 6-8 h. Upon completion, the catalyst was filtered and the residue was washed with DCM, the solvent was removed under reduced pressure to afford the residues, which were recrystallized from EtOH to give the products.

4.5.4.1. (*E*)-3-(4-bromophenyl)-1-(4-(prop-2-yn-1-yloxy)phenyl)prop-2-en-1-one **5a**, light yellow solid, yield: 86 %, m. p.: 134.5-136.0 ^{o}C, R_f = 0.46(petroleum ether/ethyl acetate = 4/1). ^{1}H NMR (400 MHz, $CDCl_3$) δ 8.14 – 7.98 (m, 2H), 7.76 (d, *J* = 15.6 Hz, 1H), 7.61 – 7.49 (m, 5H), 7.15 – 7.05 (m, 2H), 4.81 (d, *J* = 2.4 Hz, 2H), 2.59 (t, *J* = 2.4 Hz, 1H).^{13}C NMR (100 MHz, $CDCl_3$) δ 188.42, 161.34, 142.75, 133.96, 132.20, 131.67, 130.76, 129.74, 124.63, 122.33, 114.79, 77.74, 76.22, 55.90.

4.5.4.2. (*E*)-3-(3,4-dichlorophenyl)-1-(4-(prop-2-yn-1-yloxy)phenyl)prop-2-en-1-one **5b**, light yellow solid, yield: 87 %, m. p.: 143.2-144.6 ^{o}C, R_f = 0.44 (petroleum ether/ethyl acetate = 4/1). ^{1}H NMR (400 MHz, $CDCl_3$) δ 8.14 – 8.01 (m, 2H), 7.77 – 7.74 (m, 1H), 7.74 – 7.67 (d, *J* = 16.0 Hz, 1H), 7.58 – 7.52 (d, *J* = 16.0 Hz, 1H), 7.52 – 7.50 (m, 1H), 7.50 – 7.45 (m, 1H), 7.16 – 7.06 (m, 2H), 4.81 (d, *J* = 2.4 Hz, 2H), 2.59 (t, *J* = 2.4 Hz, 1H).^{13}C NMR (100 MHz, $CDCl_3$) δ 188.03, 161.46, 141.26, 135.11, 134.22, 133.29, 131.45, 130.94, 130.81, 129.67, 127.50, 123.31, 114.84, 77.70, 76.25, 55.92.

4.5.4.3. (*E*)-1-(4-(prop-2-yn-1-yloxy)phenyl)-3-(p-tolyl)prop-2-en-1-one **5c**, light yellow solid, yield: 70 %, m. p.: 102.5-103.3 ^{o}C, R_f = 0.38 (petroleum ether/ethyl acetate = 4/1). ^{1}H NMR (400 MHz, $CDCl_3$) δ 8.14 – 8.00 (m, 2H), 7.82 (d, *J* = 15.6 Hz, 1H), 7.62 – 7.52 (m, 2H), 7.51 (s, 1H), 7.25 (d, *J* = 8.0 Hz, 2H), 7.13 – 7.04 (m, 2H), 4.81 (d, *J* = 2.4 Hz, 2H), 2.59 (t, *J* = 2.4 Hz, 1H), 2.42 (s, 3H).^{13}C NMR (100 MHz, $CDCl_3$) δ 188.86, 161.13, 144.30, 140.92, 132.30, 132.02, 130.69, 129.70, 128.42, 114.70, 77.82, 76.16, 55.88, 21.54.

4.5.4.4. (*E*)-3-(3,4-difluorophenyl)-1-(4-(prop-2-yn-1-yloxy)phenyl)prop-2-en-1-one **5d**, light yellow solid, yield: 70 %, m. p.: 150.5-152.2 ^{o}C, R_f = 0.41 (petroleum ether/ethyl acetate = 4/1). ^{1}H NMR (400 MHz, $CDCl_3$) δ 8.13 – 8.01 (m, 2H), 7.72 (d, *J* = 15.6 Hz, 1H), 7.54 – 7.44 (m, 2H), 7.44 – 7.34 (m, 1H), 7.28 – 7.16 (m, 1H), 7.16 – 7.06 (m, 2H), 4.81 (d, *J* = 2.4 Hz, 2H), 2.59 (t, *J* = 2.4 Hz, 1H).^{13}C NMR (100 MHz, $CDCl_3$) δ 188.12, 161.41, 141.70, 131.52, 130.77, 125.28, 122.67, 117.97, 117.79, 116.50, 116.33, 114.83, 100.00, 77.71, 76.24, 55.91.

4.5.4.5. (*E*)-3-(4-nitrophenyl)-1-(4-(prop-2-yn-1-yloxy)phenyl)prop-2-en-1-one **5e**. yellow solid, yield: 86 %, m. p.: 172.0-1173.2 ^{o}C, R_f = 0.32 (petroleum ether/ethyl acetate = 4/1). ^{1}H NMR (400 MHz, $CDCl_3$) δ 8.31 (d, *J* = 8.7 Hz, 2H), 8.09 (d, *J* = 8.9 Hz, 2H), 7.84 (d, *J* = 15.6 Hz, 1H), 7.81 (d, *J* = 8.7 Hz, 2H), 7.67 (d, *J* = 15.7 Hz, 1H), 7.12 (d, *J* = 8.9 Hz, 2H), 4.82 (d, *J* = 2.4 Hz, 1H), 2.60 (t, *J* = 2.4 Hz, 1H).^{13}C NMR (100 MHz, $CDCl_3$) δ 187.82, 161.65, 141.23, 140.93, 131.23, 130.91, 128.87, 125.57, 124.23, 114.94, 77.64, 76.31, 55.94.

4.6. General procedure for the preparation of propargyloxy substituted coumarins **8a-c**

To a stirred solution of coumarin derivative (0.60 mmol, 1.0 eq) and K_2CO_3 (0.90 mmol, 1.5 eq) in acetone (3 mL) was added propargyl bromide (0.72 mmol, 1.2 eq) at room temperature, and then the mixture was kept at 50 ^{o}C for 4-10 h. Upon completion, K_2CO_3 was filtered and the solvent was removed under vacuum to give the residue, which was recrystallized from EtOAc to give the corresponding product. Compounds **8a-c** are known compounds [45-47] and therefore the spectra data of compound **8a** is only given here. White solid, yield: 26 %, m. p.: 119.1-120.5 ^{o}C, R_f = 0.12 (petroleum ether/ ethyl acetate = 6/1). ^{1}H NMR (400 MHz, $CDCl_3$) δ 7.67 (d, *J* = 9.5 Hz, 1H),

7.43 (d, *J* = 8.5 Hz, 1H), 7.03 – 6.86 (m, 2H), 6.31 (d, *J* = 9.5 Hz, 1H), 4.79 (d, *J* = 2.4 Hz, 2H), 2.60 (t, *J* = 2.4 Hz, 1H).^{13}C NMR (100 MHz, $CDCl_3$) δ 161.02, 160.55, 155.67, 143.28, 128.84, 113.70, 113.20, 113.09, 102.15, 76.58, 56.22.

4.7. General procedure for the preparation of substituted propargyl phenyl ethers **9a-c**

To a stirred solution of substituted phenol (1.44mmol, 1.0 eq) and K_2CO_3 (1.44 mmol, 1.0 eq) in acetone (4 mL) was added propargyl bromide (1.73 mmol, 1.2 eq) dropwise at room temperature, the mixture was kept for 5-9 h under reflux. Upon completion, K_2CO_3 was filtered and the solvent was removed under reduced pressure to give the residue, which was used directly for next step without further purification. Compounds **9a-c** are known compounds [48], so only the NMR data of compound **9a** is given below. Light yellow solid, yield: 66 %, m. p.: 77.5-78.2 ^{o}C, R_f =0.30 (petroleum ether/ethyl acetate = 6/1). ^{1}H NMR (400 MHz, $CDCl_3$) δ 7.88 (m, 1H), 7.68 – 7.53 (m, 1H), 7.34 – 7.23 (m, 1H), 7.20 – 7.04 (m, 1H), 4.88 (d, *J* = 2.4 Hz, 2H), 2.61 (t, *J* = 2.4 Hz, 1H).^{13}C NMR (100 MHz, $CDCl_3$) δ 150.77, 140.41, 133.95, 125.76, 121.45, 115.51, 77.19, 77.07, 57.22.

4.8. General procedure for the preparation of substituted propargyl anilines **10a-c**

To a solution of substituted amine (1.58 mmol, 1.0 eq) in DMF (4 mL) were added K_2CO_3 (1.58 mmol, 1.0 eq) and propargyl bromide (1.58 mmol, 1.0 eq) at room temperature. The mixture was stirred at the indicated temperature (r. t. - 50 ^{o}C) for 6 h-3 days depending on the amine used. Upon completion, EtOAc and H_2O were added, the aqueous layer was extracted with EtOAc, the combined organic layers were washed with H_2O for several times to remove the DMF, and the organic layers were washed with brine, dried over $MgSO_4$ and evaporated to give the residue, which was purified by column chromatography.

4.8.1. 4-Methoxy-*N*-(prop-2-yn-1-yl) aniline **10a**, light yellow solid, yield: 43 %, m. p.: 45.6-46.2 ^{o}C, R_f = 0.44 (petroleum ether/ethyl acetate = 4/1). ^{1}H NMR (400 MHz, $CDCl_3$) δ 6.91 – 6.78 (d, *J* = 8.0 Hz, 2H), 6.76 – 6.65 (d, *J* = 8.0 Hz, 2H), 3.93 (d, *J* = 2.4 Hz, 2H), 3.82 – 3.73 (s, 3H), 3.63 (br, 1H), 2.24 (t, *J* = 2.4 Hz, 1H).^{13}C NMR (100 MHz, $CDCl_3$) δ 152.99, 140.91, 115.13, 114.82, 81.36, 71.24, 55.72, 34.60.

4.8.2. 4-Bromo-*N*-(prop-2-yn-1-yl) aniline **10b**, light yellow solid, yield: 29 %, m. p.: 32.5-33.1 ^{o}C, R_f = 0.61 (petroleum ether/ethyl acetate = 3/1). ^{1}H NMR (400 MHz, $CDCl_3$) δ 7.33 (d, *J* = 8.9 Hz, 2H), 6.60 (d, *J* = 8.9 Hz, 2H), 3.94 (s, 3H, -N<u>H</u>- and –C<u>H</u>$_2$-), 2.25 (t, *J* = 1.6 Hz, 1H).^{13}C NMR (100 MHz, $CDCl_3$) δ 145.81, 131.99, 115.13, 110.44, 80.46, 71.57, 33.60.

4.8.3. 3-Nitro-*N*-(prop-2-yn-1-yl) aniline **10c**, yellow solid, yield: 32 %, m. p.: 86.2-87.8 ^{o}C, R_f = 0.46 (petroleum ether/ethyl acetate = 3/1). ^{1}H NMR (400 MHz, $CDCl_3$) δ 7.65 (dd, *J* = 8.1, 1.5 Hz, 1H), 7.53 (t, *J* = 2.2 Hz, 1H), 7.36 (t, *J* = 8.1 Hz, 1H), 6.99 (dd, *J* = 8.1, 2.0 Hz, 1H), 4.28 (br, 1H), 4.04 (dd, *J* = 6.1, 2.4 Hz, 2H), 2.29 (t, *J* = 2.4 Hz, 1H).^{13}C NMR (100 MHz, $CDCl_3$) δ 147.59, 129.82, 119.37, 113.23, 107.32, 79.62, 72.11, 33.43.

4.9. General procedure for the preparation of steroidal hybrids **12-18**

To a solution of azide **2** (0.27 mmol, 1.0 eq) and alkyne (0.27 mmol, 1.0 eq) in a mixture of THF (2 mL) and H_2O (2 mL) were added sodium ascorbate (0.14 mmol, 0.5 eq) and copper sulfate

pentahydrate (0.11 mmol, 0.4 eq). The mixture was stirred overnight at room temperature. Upon completion, the mixture was filtered and the filtrate was evaporated to give the residue, which was then subjected to column chromatography to afford the corresponding product.

4.9.1. Compound **12a**, yellow solid, yield: 50 %, m. p.: 191.3-192.8 ^{o}C, R_f = 0.13 (petroleum ether/acetone = 2/1). ^{1}H NMR (400 MHz, DMSO-*d*6) δ 8.18 (s, 1H), 7.64 (t, *J* = 7.7 Hz, 1H), 7.58 (d, *J* = 7.2 Hz, 1H), 7.15 (m, 2H), 5.38 (s, 1H), 5.36 (s, 2H), 5.01 (s, 2H), 4.53 (d, *J* = 5.2 Hz, 1H), 0.99 (s, 3H), 0.81 (s, 3H).^{13}C NMR (100 MHz, DMSO-*d*6) δ 183.51, 167.00, 158.28, 150.59, 139.73, 138.53, 125.57, 124.95, 123.86, 122.54, 118.07, 111.64, 75.44, 51.25, 51.00, 49.95, 47.28, 37.90, 36.73, 36.66, 35.76, 35.45, 31.59, 31.32, 30.65, 27.62, 21.89, 20.35, 19.42, 13.65. HRMS (ESI): *m*/*z* calcd for $C_{32}H_{37}N_4O_5$ $(M + H)^+$, 557.2764; found, 557.2650.

4.9.2. Compound **12b**, yellow solid, yield: 58 %, m. p.: 140.1-141.9 ^{o}C, R_f = 0.35 (petroleum ether/acetone = 2/1). ^{1}H NMR (400 MHz, DMSO-*d*6) δ 8.18 (s, 1H), 7.70 (d, *J* = 7.9 Hz, 1H), 7.64 (s, 1H), 7.20 (d, *J* = 8.2 Hz, 1H), 5.36 (s, 3H), 5.01 (s, 2H), 4.53 (s, 1H), 0.99 (s, 3H), 0.81 (s, 3H).^{13}C NMR (100 MHz, DMSO-*d*6) δ 220.09, 182.38, 166.95, 158.06, 149.05, 141.82, 139.71, 137.36, 128.10, 125.58, 124.44, 122.54, 119.51, 113.33, 75.43, 67.49, 51.25, 51.03, 49.95, 47.28, 37.89, 36.71, 36.66, 35.76, 35.55, 31.59, 31.33, 30.66, 27.61, 25.60, 21.90, 20.35, 19.38, 19.03, 13.65. HRMS (ESI): *m*/*z* calcd for $C_{32}H_{36}ClN_4O_5$ $(M + H)^+$, 591.2374; found, 591.2375.

4.9.3. Compound **12c**, yellow solid, yield: 58 %, m. p.: 141.9-143.4 ^{o}C, R_f = 0.28 (petroleum ether/acetone = 2/1). ^{1}H NMR (400 MHz, DMSO-*d*6) δ 8.17 (s, 1H), 7.82 (dd, *J* = 8.4, 2.1 Hz, 1H), 7.74 (d, *J* = 2.1 Hz, 1H), 7.14 (d, *J* = 8.4 Hz, 1H), 5.38 (d, *J* = 4.7 Hz, 1H), 5.36 (s, 2H), 5.00 (s, 2H), 4.53 (tt, *J* = 10.5, 5.2 Hz, 1H), 0.99 (s, 3H), 0.81 (s, 3H).^{13}C NMR (100 MHz, DMSO-*d*6) δ 220.09, 182.23, 166.94, 157.90, 149.42, 140.17, 139.71, 127.17, 125.58, 122.54, 119.88, 115.63, 113.76, 75.43, 67.49, 51.25, 49.95, 47.28, 37.89, 36.71, 36.66, 35.76, 35.54, 31.59, 31.33, 30.66, 27.61, 25.60, 21.89, 20.36, 19.39, 13.66. HRMS (ESI): *m*/*z* calcd for $C_{32}H_{36}BrN_4O_5$ $(M + H)^+$, 635.1869; found, 635.1859.

4.9.4. Compound **12d**, saffron solid, yield: 68 %, m. p.: 117.5-118.8 ^{o}C, R_f = 0.30 (petroleum ether/acetone = 2/1). ^{1}H NMR (400 MHz, DMSO-*d*6) δ 8.18 (s, 1H), 7.59 – 7.40 (m, 2H), 7.22 (dd, *J* = 21.6, 6.2 Hz, 1H), 5.37 (m, 3H), 5.01 (s, 2H), 4.54 (s, 1H), 0.99 (s, 3H), 0.81 (s, 3H).^{13}C NMR (100 MHz, DMSO-*d*6) δ 220.11, 182.88, 166.98, 158.32, 156.83, 146.79, 141.87, 139.71, 125.58, 124.32, 122.54, 113.00, 112.08, 111.83, 75.43, 51.25, 51.01, 49.95, 47.28, 37.89, 36.72, 36.66, 35.76, 35.51, 31.59, 31.32, 30.65, 27.62, 21.89, 20.35, 19.39, 13.65. HRMS (ESI): *m*/*z* calcd for $C_{32}H_{36}FN_4O_5$ $(M + H)^+$, 575.2670; found, 575.2673.

4.9.5. Compound **12e**, yellow solid, yield: 66 %, m. p.: 218.5-220.1 ^{o}C, R_f = 0.19 (petroleum ether/acetone = 2/1). ^{1}H NMR (400 MHz, DMSO-*d*6) δ 8.18 (s, 1H), 7.61 (t, *J* = 8.1 Hz, 1H), 7.14 (t, *J* = 8.5 Hz, 2H), 5.39 (d, *J* = 4.2 Hz, 1H), 5.35 (s, 2H), 5.01 (s, 2H), 4.54 (dd, *J* = 11.2, 5.7 Hz, 1H), 0.99 (s, 3H), 0.81 (s, 3H).^{13}C NMR (100 MHz, DMSO-*d*6) δ 220.09, 180.30, 166.96, 157.64, 151.85, 141.84, 139.72, 139.05, 131.49, 125.56, 124.80, 122.54, 115.15, 110.35, 75.44, 51.25, 51.01, 49.95, 47.28, 37.89, 36.72, 36.66, 35.76, 35.67, 31.59, 31.33, 30.65, 27.62, 21.89, 20.36, 19.40, 13.66. HRMS (ESI): *m*/*z* calcd for $C_{32}H_{36}ClN_4O_5$ $(M + H)^+$, 591.2374; found, 591.2376.

4.9.6. Compound **12f**, yellow solid, yield: 70 %, m. p.: 220.9-222.3 °C, R_f = 0.24 (petroleum ether/acetone = 2/1). ^{1}H NMR (400 MHz, DMSO-*d*6) δ 8.18 (s, 1H), 7.51 (t, *J* = 7.9 Hz, 1H), 7.30 (d, *J* = 8.0 Hz, 1H), 7.16 (d, *J* = 7.7 Hz, 1H), 5.42 – 5.37 (m, 1H), 5.35 (s, 2H), 5.01 (s, 2H), 4.60 – 4.44 (m, 1H), 0.99 (s, 3H), 0.81 (s, 3H).^{13}C NMR (100 MHz, DMSO-*d*6) δ 180.84, 166.94, 157.59, 152.27, 139.71, 138.97, 127.92, 122.54, 119.85, 116.76, 110.76, 75.43, 56.49, 51.26, 51.03, 49.96, 47.28, 37.88, 36.72, 36.66, 35.75, 35.57, 31.59, 31.32, 31.16, 30.65, 27.61, 21.89, 20.36, 19.40, 19.03, 13.65. HRMS (ESI): *m*/*z* calcd for $C_{32}H_{36}BrN_4O_5$ $(M + H)^+$, 635.1869; found, 635.1872.

4.9.7. Compound **12g**, yellow solid, yield: 65 %, m. p.: 132.1-133.9 °C, R_f = 0.22 (petroleum ether/acetone = 2/1). ^{1}H NMR (400 MHz, DMSO-*d*6) δ 8.19 (s, 1H), 7.61 (d, *J* = 8.7 Hz, 1H), 7.20 (d, *J* = 8.7 Hz, 1H), 5.38 (d, *J* = 4.9 Hz, 1H), 5.36 (s, 2H), 5.32 (s, 2H), 4.63 – 4.44 (m, 1H), 1.00 (s, 3H), 0.81 (s, 3H).^{13}C NMR (100 MHz, DMSO-*d*6) δ 220.10, 179.12, 166.96, 158.63, 146.86, 140.28, 139.71, 130.79, 129.37, 128.67, 126.23, 125.78, 124.93, 122.54, 118.10, 115.09, 75.39, 55.38, 51.25, 51.06, 49.95, 47.28, 37.95, 37.87, 36.72, 36.66, 35.76, 31.59, 31.33, 31.16, 30.65, 27.60, 21.89, 20.36, 19.40, 13.65. HRMS (ESI): *m*/*z* calcd for $C_{32}H_{35}Cl_2N_4O_5$ $(M + H)^+$, 625.1985; found, 625.1986.

4.9.8. Compound **12h**, yellow solid, yield: 51 %, m. p.: 164.2-165.7 °C, R_f = 0.17 (petroleum ether/acetone = 2/1). ^{1}H NMR (400 MHz, DMSO-*d*6) δ 8.18 (s, 1H), 7.62 (t, *J* = 7.9 Hz, 2H), 7.16 (t, *J* = 7.7 Hz, 1H), 5.39 (d, *J* = 4.8 Hz, 1H), 5.35 (s, 2H), 5.30 (s, 2H), 4.54 (dt, *J* = 10.6, 5.4 Hz, 1H), 1.00 (s, 3H), 0.81 (s, 3H).^{13}C NMR (100 MHz, DMSO-*d*6) δ 220.11, 182.24, 167.00, 159.32, 145.72, 140.01, 139.73, 125.31, 124.86, 124.04, 122.54, 121.62, 116.47, 75.39, 51.25, 51.03, 49.95, 47.28, 37.85, 36.67, 35.76, 31.59, 31.33, 31.17, 30.65, 27.60, 21.90, 20.36, 19.42, 13.66. HRMS (ESI): *m*/*z* calcd for $C_{32}H_{36}ClN_4O_5$ $(M + H)^+$, 591.2374; found, 591.2377.

4.9.9. Compound **13a**, light yellow solid, yield: 75 %, m. p.: 186.0-187.5 °C, R_f = 0.29 (petroleum ether/acetone = 2/1), ^{1}H NMR (400 MHz, DMSO-*d*6) δ 8.26 (s, 1H), 8.16 (d, *J* = 7.5 Hz, 2H), 7.88 (d, *J* = 8.6 Hz, 2H), 7.82 (s, 1H), 7.75 (s, 1H), 7.68 (dd, *J* = 15.6, 8.5 Hz, 1H), 7.58 (t, *J* = 7.5 Hz, 2H), 7.14 (d, *J* = 8.5 Hz, 2H), 5.41 (s, 2H), 5.39 (s, 1H), 5.30 (s, 2H), 4.66 – 4.45 (m, 1H), 0.97 (s, 3H), 0.76 (s, 3H).^{13}C NMR (100 MHz, DMSO-*d*6) δ 220.10, 189.38, 167.02, 160.46, 144.46, 142.91, 139.68, 138.24, 133.44, 131.29, 129.22, 128.90, 128.08, 126.61, 122.55, 120.05, 115.66, 75.45, 67.49, 61.51, 51.22, 51.04, 49.93, 47.25, 37.89, 36.65, 35.74, 31.56, 31.29, 30.64, 27.62, 21.85, 20.34, 19.37, 13.61. HRMS (ESI): *m*/*z* calcd for $C_{39}H_{42}Cl_2N_3O_5$ $(M + H)^+$, 702.2502; found, 702.2484.

4.9.10. Compound **13b**, yellow solid, yield: 54 %, m. p.: 167.4-169.1 °C, R_f = 0.27 (petroleum ether/acetone = 2/1). ^{1}H NMR (400 MHz, DMSO-*d*6) δ 8.27 (s, 3H), 7.80 (m, 4H), 7.40 (s, 2H), 7.14 (d, *J* = 7.0 Hz, 2H), 5.41 (s, 3H), 5.30 (s, 2H), 4.54 (s, 1H), 0.97 (s, 3H), 0.76 (s, 3H).^{13}C NMR (100 MHz, DMSO-*d*6) δ 187.90, 167.02, 164.19, 160.50, 144.63, 142.93, 139.68, 134.94, 131.94, 131.35, 128.05, 126.61, 122.55, 119.81, 116.32, 116.11, 115.66, 99.99, 75.46, 61.52, 51.22, 51.04, 49.93, 47.24, 37.89, 36.65, 35.75, 31.56, 31.28, 30.64, 27.61, 21.84, 20.34, 19.37, 13.59. HRMS (ESI): *m*/*z* calcd for $C_{39}H_{43}FN_3O_5$ $(M + H)^+$, 652.3187; found, 652.3184.

4.9.11. Compound **14a**, gray solid, yield: 33 %, m. p.: 204.6-205.8 °C, R_f = 0.44 (petroleum

ether/acetone = 2/1). ^{1}H NMR (400 MHz, DMSO-*d*6) δ 8.28 (s, 1H), 8.19 (d, *J* = 8.4 Hz, 2H), 8.02 (d, *J* = 15.5 Hz, 1H), 7.87 (d, *J* = 8.2 Hz, 2H), 7.76 – 7.57 (m, 3H), 7.21 (d, *J* = 8.6 Hz, 2H), 5.41 (s, 2H), 5.35 (s, 3H), 4.54 (s, 1H), 0.97 (s, 3H), 0.77 (s, 3H).^{13}C NMR (100 MHz, DMSO-*d*6) δ 220.07, 187.61, 167.00, 162.41, 142.74, 142.26, 139.68, 134.61, 132.33, 131.44, 131.21, 131.02, 126.68, 124.26, 123.18, 122.55, 115.29, 75.46, 61.68, 51.22, 51.05, 49.93, 47.25, 37.88, 36.64, 35.74, 31.56, 31.29, 31.17, 30.63, 27.62, 21.85, 20.34, 19.40, 13.61. HRMS (ESI): *m/z* calcd for $C_{39}H_{43}BrN_3O_5$ $(M + H)^+$, 712.2386; found, 712.2364 (Br^{79}) and 714.2352 (Br^{81}).

4.9.12. Compound **14b**, light yellow solid, yield: 77 %, m. p.: 153.6-154.9 °C, R_f = 0.28 (petroleum ether/acetone = 2/1). ^{1}H NMR (400 MHz, DMSO-*d*6) δ 8.26 (m, 4H), 8.09 (d, *J* = 15.6 Hz, 1H), 7.88 (s, 1H), 7.82 – 7.57 (m, 2H), 7.22 (d, *J* = 7.1 Hz, 2H), 5.41 (s, 2H), 5.36 (s, 3H), 4.53 (s, 1H), 0.96 (s, 3H), 0.76 (s, 3H). ^{13}C NMR (100 MHz, DMSO-*d*6) δ 220.06, 187.42, 166.99, 162.50, 142.74, 140.85, 139.65, 136.21, 133.02, 132.30, 131.56, 131.43, 130.88, 130.54, 129.64, 126.69, 124.39, 122.54, 115.29, 75.45, 61.68, 55.39, 51.20, 51.05, 49.91, 47.23, 39.36, 37.86, 36.68, 36.62, 35.73, 31.54, 31.26, 31.17, 30.62, 27.60, 21.84, 20.33, 19.39, 13.57. HRMS (ESI): *m/z* calcd for $C_{39}H_{42}Cl_2N_3O_5$ $(M + H)^+$, 702.2502; found, 702.2484.

4.9.13. Compound **14c**, light yellow solid, yield: 75 %, m. p.: 191.8-193.1 °C, R_f = 0.24 (petroleum ether/acetone = 2/1). ^{1}H NMR (400 MHz, DMSO-*d*6) δ 8.28 (s, 1H), 8.18 (d, *J* = 8.4 Hz, 2H), 7.92 (d, *J* = 15.5 Hz, 1H), 7.79 (d, *J* = 7.7 Hz, 2H), 7.69 (d, *J* = 15.5 Hz, 1H), 7.28 (d, *J* = 7.6 Hz, 2H), 7.21 (d, *J* = 8.6 Hz, 2H), 5.41 (s, 2H), 5.37 (s, 1H), 5.35 (s, 2H), 4.54 (s, 1H), 2.36 (s, 3H), 0.97 (s, 3H), 0.76 (s, 3H). ^{13}C NMR (100 MHz, DMSO-*d*6) δ 220.07, 187.69, 167.00, 162.26, 143.71, 142.77, 140.95, 139.68, 132.57, 131.31, 131.23, 129.99, 129.32, 126.67, 122.55, 121.30, 115.24, 75.46, 61.67, 55.39, 51.22, 51.05, 49.93, 47.25, 37.88, 36.64, 35.74, 31.56, 31.28, 31.16, 30.63, 27.61, 21.85, 21.55, 20.34, 19.39, 13.60. HRMS (ESI): *m/z* calcd for $C_{40}H_{46}N_3O_5$ $(M + H)^+$, 648.3437; found, 648.3412.

4.9.14. Compound **14d**, yellow solid, yield: 62 %, m. p.: 139.5-140.8 °C, R_f = 0.23 (petroleum ether/acetone = 2/1). ^{1}H NMR (400 MHz, DMSO-*d*6) δ 8.28 (s, 1H), 8.20 (d, *J* = 8.7 Hz, 2H), 8.15 (d, *J* = 10.6 Hz, 1H), 8.00 (d, *J* = 15.6 Hz, 1H), 7.74 (s, 1H), 7.69 (d, *J* = 15.6 Hz, 1H), 7.54 (dd, *J* = 18.7, 8.7 Hz, 1H), 7.22 (d, *J* = 8.6 Hz, 2H), 5.41 (s, 2H), 5.36 (s, 3H), 4.54 (s, 1H), 0.97 (s, 3H), 0.77 (s, 3H).^{13}C NMR (100 MHz, DMSO-*d*6) δ 220.04, 187.46, 166.99, 162.47, 142.74, 141.33, 139.68, 133.31, 131.48, 130.95, 127.25, 126.68, 123.63, 122.53, 118.49, 117.28, 115.28, 75.46, 67.48, 61.70, 51.21, 51.05, 49.93, 47.23, 37.88, 36.63, 35.73, 31.55, 31.28, 30.62, 27.61, 25.59, 21.84, 20.33, 19.38, 13.58. HRMS (ESI): *m/z* calcd for $C_{39}H_{42}F_2N_3O_5$ $(M + H)^+$, 670.3093; found, 670.3097.

4.9.15. Compound **14e**, yellow solid, yield: 57 %, m. p.: 130.5-132.3 °C, R_f = 0.20 (petroleum ether/acetone = 2/1). ^{1}H NMR (400 MHz, DMSO-*d*6) δ 8.31 (s, 1H), 8.29 (m, 2H), 8.26 – 8.13 (m, 5H), 7.80 (d, *J* = 15.6 Hz, 1H), 7.24 (d, *J* = 8.8 Hz, 2H), 5.42 (s, 2H), 5.38 (s, 1H), 5.36 (s, 2H), 4.63 – 4.45 (m, 1H), 0.98 (s, 3H), 0.77 (s, 3H).^{13}C NMR (100 MHz, DMSO-*d*6) δ 220.06, 187.50, 167.02, 162.65, 148.46, 142.69, 141.83, 140.82, 139.69, 131.63, 130.78, 130.29, 126.71, 126.48, 124.39, 122.54, 115.36, 75.46, 61.72, 51.21, 51.04, 49.93, 47.24, 37.88, 36.70, 36.64, 35.73, 31.55, 31.29, 30.63, 27.62, 21.85, 20.33, 19.40, 13.59. HRMS (ESI): *m/z* calcd for $C_{39}H_{43}N_4O_7$ $(M + H)^+$, 679.3132; found, 679.3131.

4.9.16. Compound **15a**, white solid, yield: 18 %, m. p.: 129.5-130.8 °C, R_f = 0.18 (petroleum ether/acetone = 2/1). ^{1}H NMR (400 MHz, DMSO-*d*6) δ 8.29 (s, 1H), 8.01 (d, *J* = 9.5 Hz, 1H), 7.65 (d, *J* = 8.6 Hz, 1H), 7.18 (d, *J* = 2.4 Hz, 1H), 7.04 (dd, *J* = 8.6, 2.4 Hz, 1H), 6.31 (d, *J* = 9.5 Hz, 1H), 5.42 (s, 2H), 5.40 (d, *J* = 5.1 Hz, 1H), 5.32 (s, 2H), 4.57 (dt, *J* = 10.9, 5.0 Hz, 1H), 0.99 (s, 3H), 0.81 (s, 3H).^{13}C NMR (100 MHz, DMSO-*d*6) δ 220.09, 167.06, 161.52, 160.72, 155.78, 144.77, 142.46, 139.72, 129.99, 126.83, 122.56, 113.42, 113.16, 113.07, 102.06, 75.48, 61.97, 51.25, 51.02, 49.96, 47.28, 37.91, 36.73, 36.67, 35.76, 31.60, 31.33, 30.65, 27.64, 21.90, 20.35, 19.40, 13.66. HRMS (ESI): *m*/*z* calcd for $C_{33}H_{38}N_3O_6$ $(M + H)^+$, 572.2761; found, 572.2762.

4.9.17. Compound **15b**, white solid, yield: 54 %, m. p.: 177.2-178.6 °C, R_f = 0.14 (petroleum ether/ acetone=2/1). ^{1}H NMR (400 MHz, DMSO-*d*6) δ 8.29 (s, 1H), 7.70 (d, *J* = 8.8 Hz, 1H), 7.16 (d, *J* = 2.5 Hz, 1H), 7.05 (dd, *J* = 8.8, 2.5 Hz, 1H), 6.23 (d, *J* = 1.1 Hz, 1H), 5.42 (s, 2H), 5.39 (d, *J* = 5.0 Hz, 1H), 5.32 (s, 2H), 4.64 – 4.47 (m, 1H), 2.40 (s, 4H), 0.99 (s, 3H), 0.81 (s, 3H).^{13}C NMR (100 MHz, DMSO-*d*6) δ 220.10, 167.06, 161.43, 160.59, 155.14, 153.87, 142.49, 139.72, 126.98, 126.81, 122.54, 113.84, 113.12, 111.79, 102.08, 75.47, 61.94, 51.24, 51.01, 49.95, 47.28, 39.37, 37.90, 36.72, 36.66, 35.76, 31.59, 31.33, 31.16, 30.65, 27.64, 21.89, 20.34, 19.39, 18.60, 13.65. HRMS (ESI): *m*/*z* calcd for $C_{34}H_{40}N_3O_6$ $(M + H)^+$, 586.2917; found, 586.2919.

4.9.18. Compound **16**, white solid, yield: 29 %, m. p.: 164.0-165.8 °C, R_f = 0.20 (petroleum ether/acetone = 2/1). ^{1}H NMR (400 MHz, DMSO-*d*6) δ 8.40 (s, 1H), 7.74 (dd, *J* = 7.9, 1.5 Hz, 1H), 7.70 – 7.64 (m, 1H), 7.42 (d, *J* = 7.9 Hz, 1H), 7.38 – 7.31 (m, 1H), 6.19 (s, 1H), 5.48 (s, 2H), 5.45 (s, 2H), 5.41 (d, *J* = 4.8 Hz, 1H), 4.58 (tt, *J* = 10.4, 5.1 Hz, 1H), 1.00 (s, 3H), 0.81 (s, 3H).^{13}C NMR (100 MHz, DMSO-*d*6) δ 167.06, 164.75, 161.99, 153.25, 141.47, 139.73, 133.32, 127.25, 124.71, 123.25, 122.57, 116.98, 115.56, 91.86, 75.52, 63.13, 51.25, 49.96, 47.28, 37.94, 36.74, 36.67, 35.76, 31.60, 31.33, 30.65, 27.67, 21.90, 20.36, 19.41, 13.66. HRMS (ESI): *m*/*z* calcd for $C_{33}H_{38}N_3O_6$ $(M + H)^+$, 572.2761; found, 572.2759.

4.9.19. Compound **17a**, light brown solid, yield: 78 %, m. p.: 153.2-154.7 °C, R_f = 0.31 (petroleum ether/acetone = 2/1). ^{1}H NMR (400 MHz, DMSO-*d*6) δ 8.26 (s, 1H), 7.87 (d, *J* = 7.7 Hz, 1H), 7.68 (t, *J* = 7.5 Hz, 1H), 7.60 (d, *J* = 8.4 Hz, 1H), 7.15 (t, *J* = 7.6 Hz, 1H), 5.41 (d, 5H, overlapped), 4.57 (s, 1H), 1.01 (s, 3H), 0.81 (s, 3H). ^{13}C NMR (100 MHz, DMSO-*d*6) δ 167.06, 150.97, 142.30, 140.26, 139.76, 135.46, 134.74, 127.64, 126.80, 125.39, 122.55, 121.41, 116.02, 75.48, 62.89, 51.25, 51.02, 49.96, 47.29, 37.93, 36.75, 36.68, 35.76, 31.59, 31.33, 30.66, 27.66, 21.90, 20.36, 19.43, 13.66. HRMS (ESI): *m*/*z* calcd for $C_{30}H_{37}N_4O_6$ $(M + H)^+$, 549.2713; found, 549.2713.

4.9.20. Compound **17b**, yellow solid, yield: 80 %, m. p.: 176.9-178.2 °C, R_f = 0.42 (petroleum ether/acetone=2/1). ^{1}H NMR (400 MHz, DMSO-*d*6) δ 8.23 (s, 1H), 7.47 (d, *J* = 8.8 Hz, 2H), 7.03 (d, *J* = 8.8 Hz, 2H), 5.40 (s, 3H), 5.19 (s, 2H), 4.58 (dt, *J* = 10.6, 4.8 Hz, 1H), 1.02 (s, 3H), 0.81 (s, 3H).^{13}C NMR (100 MHz, DMSO-*d*6) δ 220.09, 167.09, 157.73, 142.89, 139.75, 132.61, 126.58, 122.56, 117.53, 112.76, 75.49, 61.63, 51.26, 50.98, 49.97, 47.28, 39.38, 37.94, 36.75, 36.68, 35.76, 31.60, 31.34, 30.66, 27.67, 21.90, 20.36, 19.43, 13.66. HRMS (ESI): *m*/*z* calcd for $C_{30}H_{37}BrN_3O_4$ $(M + H)^+$, 582.1967; found, 582.1953.

4.9.21. Compound **17c**, yellow solid, yield: 69 %, m. p.: 177.8-179.5 ^{o}C, R_f = 0.97 (petroleum ether/acetone = 2/1). ^{1}H NMR (400 MHz, DMSO-*d*6) δ 8.21 (s, 1H), 7.10 (d, *J* = 8.3 Hz, 2H), 6.93 (d, *J* = 8.3 Hz, 2H), 5.40 (s, 3H, overlapped), 5.13 (s, 2H), 4.58 (dd, *J* = 10.7, 5.7 Hz, 1H), 2.24 (s, 3H), 1.02 (s, 3H), 0.81 (s, 3H).^{13}C NMR (100 MHz, DMSO-*d*6) δ 220.10, 167.12, 156.36, 139.77, 130.29, 129.95, 126.36, 122.56, 115.00, 75.48, 61.39, 51.26, 50.95, 49.97, 47.28, 37.95, 36.76, 36.68, 35.76, 31.60, 31.34, 30.66, 27.67, 21.90, 20.55, 20.36, 19.43, 13.66. HRMS (ESI): *m*/*z* calcd for $C_{31}H_{40}N_3O_4$ $(M + H)^+$, 518.3019; found, 518.3021.

4.9.22. Compound **18a**, light brown solid, yield: 56 %, m. p.: 149.2-150.0 ^{o}C, R_f = 0.25 (petroleum ether/acetone = 2/1). ^{1}H NMR (400 MHz, DMSO-*d*6) δ 7.92 (s, 1H), 6.70 (d, *J* = 8.1 Hz, 2H), 6.59 (d, *J* = 8.1 Hz, 2H), 5.66 (br, 1H), 5.40 (s, 1H), 5.34 (s, 2H), 4.55 (d, *J* = 5.5 Hz, 1H), 4.28 (s, 2H), 3.63 (s, 3H), 1.01 (s, 3H), 0.81 (s, 3H).^{13}C NMR (100 MHz, DMSO-*d*6) δ 220.13, 167.16, 153.62, 139.76, 133.63, 122.54, 120.19, 114.94, 113.94, 75.36, 55.70, 51.24, 50.87, 49.95, 47.28, 37.94, 36.75, 36.67, 35.76, 31.59, 31.32, 30.65, 27.66, 21.90, 20.35, 19.42, 13.65. HRMS (ESI): *m*/*z* calcd for $C_{31}H_{41}N_4O_4$ $(M + H)^+$, 533.3128; found, 533.3129.

4.9.23. Compound **18b**, yellowish solid, yield: 80 %, m. p.: 95.8-96.6 ^{o}C, R_f = 0.29 (petroleum ether/acetone = 2/1). ^{1}H NMR (400 MHz, DMSO-*d*6) δ 7.95 (s, 1H), 7.19 (d, *J* = 7.7 Hz, 2H), 6.60 (d, *J* = 7.7 Hz, 2H), 6.39 (s, 1H), 5.41 (s, 1H), 5.34 (s, 2H), 4.55 (s, 1H), 4.31 (s, 2H), 1.01 (s, 3H), 0.81 (s, 3H).^{13}C NMR (100 MHz, DMSO-*d*6) δ 220.13, 167.12, 148.02, 139.75, 131.79, 129.37, 128.68, 122.55, 114.73, 107.12, 75.37, 51.25, 50.89, 49.96, 47.28, 38.71, 37.94, 36.74, 36.67, 35.76, 31.59, 31.33, 30.66, 27.65, 21.90, 20.36, 19.42, 13.65. HRMS (ESI): *m*/*z* calcd for $C_{30}H_{38}BrN_4O_3$ $(M + H)^+$, 581.2127; found, 581.2128.

4.9.24. Compound **18c**, yellow solid, yield: 54 %, m. p.: 183.9-185.8 ^{o}C, R_f = 0.20 (petroleum ether/acetone = 2/1). ^{1}H NMR (400 MHz, DMSO-*d*6) δ 8.00 (s, 1H), 7.44 (t, *J* = 2.2 Hz, 1H), 7.35 (m, 2H), 7.12 – 7.02 (m, 1H), 6.94 (t, *J* = 5.9 Hz, 1H), 5.39 (d, *J* = 4.9 Hz, 1H), 5.35 (s, 2H), 4.54 (m, 1H), 4.43 (d, *J* = 5.6 Hz, 2H), 0.99 (s, 3H), 0.81 (s, 3H).^{13}C NMR (100 MHz, DMSO-*d*6) δ 220.13, 167.11, 149.84, 149.23, 145.39, 139.73, 130.42, 124.72, 122.54, 119.01, 110.66, 106.19, 75.36, 51.24, 50.92, 49.95, 47.28, 38.52, 37.91, 36.73, 36.66, 35.76, 31.59, 31.32, 30.65, 27.63, 21.90, 20.35, 19.40, 13.65. HRMS (ESI): *m*/*z* calcd for $C_{30}H_{38}N_5O_5$ $(M + H)^+$, 548.2873; found, 548.2873.

4.10. Synthesis of 5-Fu linked dimers **20** and **21**

4.10.1. Synthesis of dipropargyl substituted 5-Fu **11**

To a stirred solution of 5-Fu (100 mg, 0.77 mmol, 1.0 eq) in DMF (10 mL) was added K_2CO_3 (106 mg, 0.77 mmol, 1.0 eq) at room temperature. 30 min later, propargyl bromide (184 μL, 2.31 mmol, 3.0 eq) was added to the above solution. The mixture was stirred at room temperature for 1.5 h. Upon completion, EtOAc and H_2O were added, the aqueous layer was extracted with EtOAc, the combined organic layers were washed with H_2O for several times to remove the DMF, and the organic layers were washed with brine, dried over $MgSO_4$ and evaporated to give the residue, which was recrystallized from EtOH (2 mL) to give the product, white solid, yield: 51 %, m. p.: 96.3-97.8 ^{o}C, R_f = 0.33 (petroleum ether/acetone = 2/1). ^{1}H NMR (400 MHz, $CDCl_3$) δ 7.63 (d, $J_{C\text{-}F}$ = 5.3 Hz, 1H), 4.76 (d, *J* = 2.3 Hz, 2H), 4.64 (d, *J* = 2.5 Hz, 2H), 2.59 (t, *J* = 2.6 Hz, 1H), 2.23 (t, *J* = 2.4 Hz, 1H).^{13}C NMR (100 MHz, $CDCl_3$) δ 156.08 (d, $J_{C\text{-}F}$ = 26.1 Hz), 148.83, 140.18 (d, $J_{C\text{-}F}$ = 237.4 Hz),

125.16 (d, $J_{C\text{-}F}$ = 33.6 Hz), 77.13, 76.69, 75.33, 71.41, 38.07, 31.17.

4.10.2. Synthesis of 2-nitrobenzyl azide **19**

2-Chlorobenzyl chloride (158 μL, 1.24 mmol, 1.0 eq) and NaN_3 (97 mg, 1.49 mmol, 1.2 eq) were dissolved in DMSO (4 mL) at room temperature. The mixture was kept for about 3 h at 30 ^oC. Upon completion, Et_2O and H_2O were added, the aqueous layer was extracted with Et_2O, the combined organic layers were washed with H_2O for several times to remove the DMSO, and the organic layers were washed with brine, dried over $MgSO_4$ and evaporated to give the yellow oil, R_f = 0.67 (petroleum ether/ethyl acetate = 4/1). ^1H NMR (400 MHz, $CDCl_3$) δ 7.56 – 7.38 (m, 2H), 7.38 (m, 2H), 4.52 (s, 2H). ^{13}C NMR (100 MHz, $CDCl_3$) δ 133.79, 133.33, 130.05, 129.80, 129.67, 127.19, 52.29.

4.10.3. Synthesis of 5-Fu linked steroidal dimer **20**

To a solution of azide **2** (180 mg, 0.48 mmol, 1.0 eq) and alkyne **11** (50 mg, 0.24 mmol, 0.5 eq) in a mixture of THF (3 mL) and H_2O (3 mL) were added sodium ascorbate (48mg, 0.24 mmol, 0.5 eq) and copper sulfate pentahydrate (48 mg, 0.19 mmol, 0.4 eq). The mixture was stirred overnight at room temperature. Upon completion, the mixture was filtered and the filtrate was evaporated to the residue, which was subjected to column chromatography to afford the product. White solid, yield: 38 %, m. p.: 183.8-185.1 ^oC, R_f = 0.30 (petroleum ether/acetone = 2/1). ^1H NMR (400 MHz, DMSO-*d*6) δ 8.39 (s, 1H), 8.14 (s, 1H), 8.00 (s, 1H), 5.52 – 5.22 (m, 6H), 5.08 (s, 2H), 5.02 (s, 2H), 4.57 (s, 2H), 1.02 (s, 6H), 0.81 (s, 6H).^{13}C NMR (101 MHz, DMSO-*d*6) δ 220.03, 167.06, 167.03, 157.00, 156.74, 149.69, 142.50, 142.35, 140.75, 139.77, 138.48, 129.66, 129.33, 125.81, 125.62, 122.54, 75.47, 75.43, 51.29, 50.97, 50.87, 49.99, 47.28, 44.34, 37.95, 36.77, 36.68, 35.75, 31.61, 31.34, 30.67, 27.67, 21.89, 20.37, 19.41, 13.64. HRMS (ESI): *m/z* calcd for $C_{52}H_{66}FN_8O_8$ $(M + H)^+$, 949.4988; found, 949.4990.

4.10.4. Synthesis of 5-Fu linked non-steroidal dimer **21**

To a solution of azide **19** (128 mg, 0.76 mmol, 2.0 eq) and alkyne **11** (79 mg, 0.38 mmol, 1.0 eq) in a mixture of THF (2 mL) and H_2O (2 mL) were added sodium ascorbate (76mg, 0.38 mmol, 1.0 eq) and copper sulfate pentahydrate (76 mg, 0.30 mmol, 0.79 eq). The mixture was stirred overnight at room temperature. Upon completion, the mixture was filtered and the filtrate was evaporated to the residue, which was subjected to column chromatography to afford the product. White solid, yield: 14 %, m. p.: 59.1-60.9 ^oC, R_f = 0.10 (petroleum ether/acetone = 2/1). ^1H NMR (400 MHz, DMSO-*d*6) δ 8.34 (d, *J* = 6.3 Hz, 1H), 8.17 (s, 1H), 8.03 (s, 1H), 7.52 (d, *J* = 7.6 Hz, 2H), 7.46 – 7.28 (m, 4H), 7.20 (dd, *J* = 16.1, 7.1 Hz, 2H), 5.69 (s, 2H), 5.66 (s, 2H), 5.06 (s, 2H), 5.00 (s, 2H).^{13}C NMR (100 MHz, DMSO-*d*6) δ 157.08, 156.82, 149.71, 142.64, 142.48, 140.75, 138.48, 133.71, 133.59, 133.09, 133.03, 130.99, 130.85, 130.74, 130.67, 130.10, 130.07, 129.69, 129.36, 128.21, 128.19, 124.80, 124.54, 51.10, 50.96, 44.32, 37.07, 31.16. HRMS (ESI): *m/z* calcd for $C_{32}H_{36}ClN_4O_5$ $(M + H)^+$, 591.2374; found, 591.1072.

4.11. Biological testing

The MTT assay, analysis of cell cycle distribution, detection of apoptosis and mitochondrial membrane potential were carried out following our previously reported method [17]. The assay of LSD1 inhibition was performed according to the methods previously published [5]. Therefore,

no details are given here.

4.12. Molecular docking studies

The protein complexes used for this study were obtained from protein data bank (PDB code: 2H94), and all water molecules were eliminated. Hydrogen and partial charges were added by the protonate 3D program of MOE2014; Energy minimization of the ligands was carried out using energy minimize program of MOE. Default parameter settings generated by the program of MOE were used for docking.

Acknowledgement

We are grateful for the financial support from the Natural Science Foundation of China (No. 21372206) and the Development Foundation of Priority, Ministry of Education (No. 20134101130001). Bin Yu and Xiao-Jing Shi express their thanks to the outstanding PhD training program of Zhengzhou University for financial support. Bin Yu designed this project, analyzed the data and wrote the manuscript; Ping-Ping Qi performed the chemical synthesis of reported compounds; Xiao-Jing Shi carried out most of the biology experiments; Ruilei Huang carried out the docking studies; Dr. Yi-Chao Zheng performed the LSD1 inhibition assay; Hao Guo provided MS analysis services of some compounds; *Prof.* De-Quan Yu and *Prof.* Hong-Min Liu, as corresponding authors, proofread this manuscript and approved the final submission.

References

[1] C. Viegas-Júnior, A. Danuello, V. da Silva Bolzani, E. J. Barreiro, C. A. M. Fraga. Molecular hybridization: a useful tool in the design of new drug prototypes. Curr. Med. Chem. 14 (2007) 1829-1852.

[2] P. B. Sampson, Y. Liu, B. Forrest, G. Cumming, S.-W. Li, N. K. Patel, L. Edwards, R. Laufer, M. Feher, F. Ban, D. E. Awrey, G. Mao, O. Plotnikova, R. Hodgson, I. Beletskaya, J. M. Mason, X. Luo, V. Nadeem, X. Wei, R. Kiarash, B. Madeira, P. Huang, T. W. Mak, G. Pan, H. W. Pauls. The Discovery of Polo-Like Kinase 4 Inhibitors: Identification of (1R,2S)-2-(3-((E)-4-(((cis)-2,6-Dimethylmorpholino)methyl)styryl)-1H-indazol-6-yl)-5′-methoxyspiro[cyclopropane-1,3′-indolin]-2′-one (CFI-400945) as a Potent, Orally Active Antitumor Agent. J. Med. Chem. 58 (2015) 147-169.

[3] B. Yu, Z. Yu, P.-P. Qi, D.-Q. Yu, H.-M. Liu. Discovery of orally active anticancer candidate CFI-400945 derived from biologically promising spirooxindoles: Success and challenges. Eur. J. Med. Chem. 95 (2015) 35-40.

[4] M. Videnović, D. M. Opsenica, J. C. Burnett, L. Gomba, J. E. Nuss, Ž. Selaković, J. Konstantinović, M. Krstić, S. Šegan, M. Zlatović, R. J. Sciotti, S. Bavari, B. A. Šolaja. Second Generation Steroidal 4-Aminoquinolines Are Potent, Dual-Target Inhibitors of the Botulinum Neurotoxin Serotype A Metalloprotease and P. falciparum Malaria. J. Med. Chem. 57 (2014) 4134-4153.

[5] Y.-C. Zheng, Y.-C. Duan, J.-L. Ma, R.-M. Xu, X. Zi, W.-L. Lv, M.-M. Wang, X.-W. Ye, S. Zhu, D. Mobley, Y.-Y. Zhu, J.-W. Wang, J.-F. Li, Z.-R. Wang, W. Zhao, H.-M. Liu. Triazole–Dithiocarbamate Based Selective Lysine Specific Demethylase 1 (LSD1) Inactivators Inhibit Gastric Cancer Cell Growth, Invasion, and Migration. J. Med. Chem. 56 (2013) 8543-8560.

[6] X.-W. Ye, Y.-C. Zheng, Y.-C. Duan, M.-M. Wang, B. Yu, J.-L. Ren, J.-L. Ma, E. Zhang, H.-M. Liu. Synthesis

and biological evaluation of coumarin-1,2,3-triazole-dithiocarbamate hybrids as potent LSD1 inhibitors. MedChemComm 5 (2014) 650-654.

[7] L.-Y. Ma, Y.-C. Zheng, S.-Q. Wang, B. Wang, Z.-R. Wang, L.-P. Pang, M. Zhang, J.-W. Wang, L. Ding, J. Li, C. Wang, B. Hu, Y. Liu, X.-D. Zhang, J.-J. Wang, Z.-J. Wang, W. Zhao, H.-M. Liu. Design, Synthesis, and Structure–Activity Relationship of Novel LSD1 Inhibitors Based on Pyrimidine–Thiourea Hybrids As Potent, Orally Active Antitumor Agents. J. Med. Chem. 58 (2015) 1705-1716.

[8] Y. Jiang, T. Miyazaki, A. Honda, T. Hirayama, S. Yoshida, N. Tanaka, Y. Matsuzaki. Apoptosis and inhibition of the phosphatidylinositol 3-kinase/Akt signaling pathway in the anti-proliferative actions of dehydroepiandrosterone. J. Gastroenterol 40 (2005) 490-497.

[9] B. Yu, X.-J. Shi, P.-P. Qi, D.-Q. Yu, H.-M. Liu. Design, synthesis and biological evaluation of novel steroidal spiro-oxindoles as potent antiproliferative agents. J. Steroid Biochem. Mol. Biol. 141 (2014) 121-134.

[10] B. Yu, P.-P. Qi, X.-J. Shi, L.-H. Shan, D.-Q. Yu, H.-M. Liu. Discovery of novel steroidal pyran–oxindole hybrids as cytotoxic agents. Steroids 88 (2014) 44-52.

[11] B. Yu, D.-Q. Yu, H.-M. Liu. Spirooxindoles: Promising scaffolds for anticancer agents. Eur. J. Med. Chem. 97 (2015) 673-698.

[12] J.-L. Ren, X.-Y. Zhang, B. Yu, X.-X. Wang, K.-P. Shao, X.-G. Zhu, H.-M. Liu. Discovery of novel AHLs as potent antiproliferative agents. European Journal of Medicinal Chemistry 93 (2015) 321-329.

[13] T. Shiokawa, Y. Hattori, K. Kawano, Y. Ohguchi, H. Kawakami, K. Toma, Y. Maitani. Effect of Polyethylene Glycol Linker Chain Length of Folate-Linked Microemulsions Loading Aclacinomycin A on Targeting Ability and Antitumor Effect In vitro and In vivo. Clin. Cancer Res. 11 (2005) 2018-2025.

[14] J.-L. Ren, E. Zhang, X.-W. Ye, M.-M. Wang, B. Yu, W.-H. Wang, Y.-Z. Guo, H.-M. Liu. Design, synthesis and antibacterial evaluation of novel AHL analogues. Bioorg. Med. Chem. Lett. 23 (2013) 4154-4156.

[15] G. de Miguel, M. Wielopolski, D. I. Schuster, M. A. Fazio, O. P. Lee, C. K. Haley, A. L. Ortiz, L. Echegoyen, T. Clark, D. M. Guldi. Triazole Bridges as Versatile Linkers in Electron Donor–Acceptor Conjugates. J. Am. Chem. Soc. 133 (2011) 13036-13054.

[16] J.-M. Xu, E. Zhang, X.-J. Shi, Y.-C. Wang, B. Yu, W.-W. Jiao, Y.-Z. Guo, H.-M. Liu. Synthesis and preliminary biological evaluation of 1,2,3-triazole-Jaspine B hybrids as potential cytotoxic agents. Eur. J. Med. Chem. 80 (2014) 593-604.

[17] B. Yu, X.-J. Shi, Y.-F. Zheng, Y. Fang, E. Zhang, D.-Q. Yu, H.-M. Liu. A novel [1,2,4] triazolo [1,5-a] pyrimidine-based phenyl-linked steroid dimer: Synthesis and its cytotoxic activity. Eur. J. Med. Chem. 69 (2013) 323-330.

[18] L.-H. Huang, Y.-F. Zheng, Y.-Z. Lu, C.-J. Song, Y.-G. Wang, B. Yu, H.-M. Liu. Synthesis and biological evaluation of novel steroidal[17,16-d][1,2,4]triazolo[1,5-a]pyrimidines. Steroids 77 (2012) 710-715.

[19] B. Yu, E. Zhang, X.-N. Sun, J.-L. Ren, Y. Fang, B.-L. Zhang, D.-Q. Yu, H.-M. Liu. Facile synthesis of novel D-ring modified steroidal dienamides via rearrangement of 2H-pyrans. Steroids 78 (2013) 494-499.

[20] B. Yu, X.-J. Shi, J.-l. Ren, X.-N. Sun, P.-P. Qi, Y. Fang, X.-W. Ye, M.-M. Wang, J.-W. Wang, E. Zhang, D.-Q. Yu, H.-M. Liu. Efficient construction of novel D-ring modified steroidal dienamides and their cytotoxic activities. Eur. J. Med. Chem. 66 (2013) 171-179.

[21] B.-L. Zhang, E. Zhang, L.-P. Pang, L.-X. Song, Y.-F. Li, B. Yu, H.-M. Liu. Design and synthesis of novel D-ring fused steroidal heterocycles. Steroids 78 (2013) 1200-1208.

[22] B. Yu, X.-N. Sun, X.-J. Shi, P.-P. Qi, Y. Fang, E. Zhang, D.-Q. Yu, H.-M. Liu. Stereoselective synthesis of novel antiproliferative steroidal (*E, E*) dienamides through a cascade aldol/cyclization process. Steroids

78 (2013) 1134-1140.

[23] Y.-L. Zhang, Y.-F. Li, Y.-K. Shi, B. Yu, G.-C. Zhang, P.-P. Qi, D.-J. Fu, L.-H. Shan, H.-M. Liu. Efficient three-component one-pot synthesis of steroidal polysubstituted anilines. Steroids 2015, in press. DOI: 10.1016/j.steroids.2015.07.005.

[24] D. M. Stacy, S. T. Le Quement, C. L. Hansen, J. W. Clausen, T. Tolker-Nielsen, J. W. Brummond, M. Givskov, T. E. Nielsen, H. E. Blackwell. Synthesis and biological evaluation of triazole-containing N-acyl homoserine lactones as quorum sensing modulators. Org. Biomol. Chem. 11 (2013) 938-954.

[25] Z. Nowakowska. A review of anti-infective and anti-inflammatory chalcones. Eur. J. Med. Chem. 42 (2007) 125-137.

[26] D. K. Mahapatra, S. K. Bharti, V. Asati. Chalcone scaffolds as anti-infective agents: Structural and molecular target perspectives. Eur. J. Med. Chem. 101 (2015) 496-524.

[27] D. K. Mahapatra, S. K. Bharti, V. Asati. Anti-cancer chalcones: Structural and molecular target perspectives. Eur. J. Med. Chem. 98 (2015) 69-114.

[28] D. K. Mahapatra, V. Asati, S. K. Bharti. Chalcones and their therapeutic targets for the management of diabetes: Structural and pharmacological perspectives. Eur. J. Med. Chem. 92 (2015) 839-865.

[29] S. Emami, S. Dadashpour. Current developments of coumarin-based anti-cancer agents in medicinal chemistry. Eur. J. Med. Chem. 102 (2015) 611-630.

[30] A. Thakur, R. Singla, V. Jaitak. Coumarins as anticancer agents: A review on synthetic strategies, mechanism of action and SAR studies. Eur. J. Med. Chem. 101 (2015) 476-495.

[31] R. S. Keri, S. B.S, B. M. Nagaraja, M. A. Santos. Recent progress in the drug development of coumarin derivatives as potent antituberculosis agents. Eur. J. Med. Chem. 100 (2015) 257-269.

[32] B. Yu, X.-N. Sun, X.-J. Shi, P.-P. Qi, Y.-C. Zheng, D.-Q. Yu, H.-M. Liu. Efficient synthesis of novel antiproliferative steroidal spirooxindoles via the [3+2] cycloaddition reactions of azomethine ylides. Steroids 102 (2015) 92-100.

[33 Y. Nakayama, H. Sakamoto, K. Satoh, T. Yamamoto. Tamoxifen and gonadal steroids inhibit colon cancer growth in association with inhibition of thymidylate synthase, survivin and telomerase expression through estrogen receptor beta mediated system. Cancer Lett. 161 (2000) 63-71.

[34] J. Song, L. Hou, C. Ju, J. Zhang, Y. Ge, W. Yue. Isatin inhibits proliferation and induces apoptosis of SH-SY5Y neuroblastoma cells in vitro and in vivo. Eur. J. Pharmacol. 702 (2013) 235-241.

[35] L. Hou, C. Ju, J. Zhang, J. Song, Y. Ge, W. Yue. Antitumor effects of Isatin on human neuroblastoma cell line (SH-SY5Y) and the related mechanism. Eur. J. Pharmacol. 589 (2008) 27-31.

[36] W.-M. Zhou, R.-R. He, J.-T. Ye, N. Zhang, D.-Y. Liu. Synthesis and Biological Evaluation of New 5-Fluorouracil-Substituted Ampelopsin Derivatives. Molecules 15 (2010) 2114-2123.

[37] Z.-Y. Tian, G.-J. Du, S.-Q. Xie, J. Zhao, W.-Y. Gao, C.-J. Wang. Synthesis and Bioevaluation of 5-Fluorouracil Derivatives. Molecules 12 (2007) 2450-2457.

[38] G. K. Schwartz, M. A. Shah. Targeting the Cell Cycle: A New Approach to Cancer Therapy. J. Clin. Oncol. 23 (2005) 9408-9421.

[39] E. Gottlieb, S. M. Armour, M. H. Harris, C. B. Thompson. Mitochondrial membrane potential regulates matrix configuration and cytochrome c release during apoptosis. Cell Death Differ. 10 (2003) 709-717.

[40] J. H. Schulte, S. Lim, A. Schramm, N. Friedrichs, J. Koster, R. Versteeg, I. Ora, K. Pajtler, L. Klein-Hitpass, S. Kuhfittig-Kulle, E. Metzger, R. Schüle, A. Eggert, R. Buettner, J. Kirfel. Lysine-Specific Demethylase 1 Is Strongly Expressed in Poorly Differentiated Neuroblastoma: Implications for Therapy.

Cancer Res. 69 (2009) 2065-2071.

[41] Y.-C. Zheng, J. Ma, Z. Wang, J. Li, B. Jiang, W. Zhou, X. Shi, X. Wang, W. Zhao, H.-M. Liu. A Systematic Review of Histone Lysine-Specific Demethylase 1 and Its Inhibitors. Med. Res. Rev. 35 (2015) 1032-1071.

[42] F. González-Bobes, N. Kopp, L. Li, J. Deerberg, P. Sharma, S. Leung, M. Davies, J. Bush, J. Hamm, M. Hrytsak. Scale-up of Azide Chemistry: A Case Study. Org. Process Res. Dev. 16 (2012) 2051-2057.

[43] R. E. Conrow, W. D. Dean. Diazidomethane Explosion. Org. Process Res. Dev. 12 (2008) 1285-1286.

[44] C. Niu, G. Li, A. Tuerxuntayi, H. A. Aisa. Synthesis and Bioactivity of New Chalcone Derivatives as Potential Tyrosinase Activator Based on the Click Chemistry. Chin. J. Chem. 33 (2015) 486-494.

[45] J. Liu, P. T. Pham, E. V. Skripnikova, S. Zheng, L. N. J. Lovings, Y. Wang, N. Goyal, S. M. Bellow, L. M. Mensah, A. J. Chatters, M. R. Bratton, T. E. Wiese, M. Zhao, G. Wang, M. Foroozesh. A Ligand-Based Drug Design. Discovery of 4-Trifluoromethyl-7, 8-pyranocoumarin as a Selective Inhibitor of Human Cytochrome P450 1A2. J. Med. Chem. 58 (2015) 6481-6493.

[46] X. Li, X. Chen, J. Yuan, Y. Liu, P. Li, L. Qu, Y. Zhao. An Efficient Synthesis of 1, 2, 3-Triazole Bridge-Connected Phosphonate Derivatives of Coumarin. Phosphorus Sulfur Silicon Relat. Elem. 190 (2015) 961-971.

[47] R. Pingaew, A. Saekee, P. Mandi, C. Nantasenamat, S. Prachayasittikul, S. Ruchirawat, V. Prachayasittikul. Synthesis, biological evaluation and molecular docking of novel chalcone–coumarin hybrids as anticancer and antimalarial agents. Eur. J. Med. Chem. 85(2014) 65-76.

[48] J. B. He, H. F. He, L. L. Zhao, L. Zhang, G. Y. You, L. L. Feng, J. Wan, H. W. He. Synthesis and antifungal activity of 5-iodo-1,4-disubstituted-1,2,3-triazole derivatives as pyruvate dehydrogenase complex E1 inhibitors, Bioorg. Med. Chem. 23 (2015) 1395-1401.

[49] Y. Chen, Y. Yang; F. Wang, K. Wan, K. Yamane, Y. Zhang, M. Lei. Crystal structure of human histone lysine-specific demethylase1 (LSD1). Proc. Natl. Acad. Sci. U.S.A. 103 (2006), 13956-13961.

Highlights

- Steroidal hybrids **12a-x** were synthesized using the molecular hybridization approach.
- Compounds **12a-x** showed varied cytotoxicity against the tested cancer cell lines
- Compounds with terminal isatin scaffold were sensitive to SH-SY5Y cells possibly through LSD1 inactivation
- Compound **12g** potently inhibited growth of SH-SY5Y cells (IC_{50} = 4.06 μM)
- Compound **12g** arrested cell cycle at G2/M phase, induced apoptosis and decreased MMP.
- Docking simulations were performed to show the binding models of compound **12g** in the active site of LSD1.